Note to Editor

Following the subsequent discussion with Nigel Penna we decided to exclude the mention of the issue related to the “synth_err” parameter and synthetic signal introduction through nominals both from the publication and supplementary material. We believe that the issue is of very low importance.

Also, we made a few minor language enhancements.

Best,

Bogdan Matviichuk

Response to Reviewer 1's remarks on "Estimating ocean tide loading displacements with GPS and GLONASS" se-2020-22

We thank the reviewer and editor for constructive remarks which we respond to below in **bold.**

NOTE: On additional check we found some minor errors in our plotting routine which slightly affected figures 3, 6, 9, 10, 11 and their supplementary versions. We updated the figures and their analysis. These changes do not affect the conclusions.

The key updates are:

- **Fig 3: GPS AR (JPL) the variance in up is smaller by ~1.3 mm for S2 and 1 mm for K1 but larger by ~2.5 mm for K2**
- **Fig 6. CODE GPS a ~1 mm bias in S2 appears for solutions with cutoff angle >= 10 while median values change marginally.**
- **Fig 9. GPS (JPL) a ~0.7 mm bias in S2 east appears. The variances of K1 and K2 become smaller by ~2 mm**
- **Fig 10. GPS AR (JPL) shows a clearer linear dependency with cutoff angle.**
- **Fig 11. A constant ~0.3 mm S2 east bias appears**

Why, for example, is the OTL signal removed a priori in the GipsyX PPP solutions (using FES2004_Gbe, cf. Line 106)? Later, the OTL signal is added back in (imperfectly) using HARDISP (Line 140). Why not simply turn off the OTL model in GipsyX and attempt to recover the full expression of OTL, thus removing any doubt that the a priori model is somehow favoured via constraint? In this scenario, one could adopt a less constrained random walk (RW) for recovery of the position. Why indeed does the 3.2 mm/sqrt(s) recipe from Penna et al. (2015) again emerge as the optimal constraint for the RW position estimate? Figure 2 does not seem to suggest that the amplitudes of the recovered OTL constituents become unbounded with higher process noise. Indeed, they seem to stabilize. One wonders what the outcome would be with a more disruptive estimation strategy that allows the position to move more freely and independently (with no background OTL model). Perhaps I am missing something here, and would of course invite the authors to clarify.

The approach we use is the same as adopted by Penna et al (2015). This approach is adopted to 1) remove in a convenient way the companion tides using the hardisp routine and 2) it reduces time series variability and hence allows for the selection of a tighter time series process noise which helps reduce noise.

Our finding of the optimal process noise setting is the same as Penna et al (2015). This is not surprising to us given that we use a similar site which is therefore subject to very similar site noise, tropospheric variations and OTL. The key difference is the time period and the addition of GLONASS data. That the findings on the optimal parameters are the same as Penna et al suggests that data noise or product noise is less important than the geophysical signal. Note that we choose a slightly conservative process noise that allows for sites to have significant freedom. On additional testing, we found that the overall vector difference for M2 between the approach used in Penna et al. (2015) and approach with OTL not modelled during processing run is ~0.1 mm (Fig. R1), however, this difference also includes phase variations due to companion tides and hence this is an upper bound on the difference.

Given this is a standard and widely used approach we do not modify the manuscript.

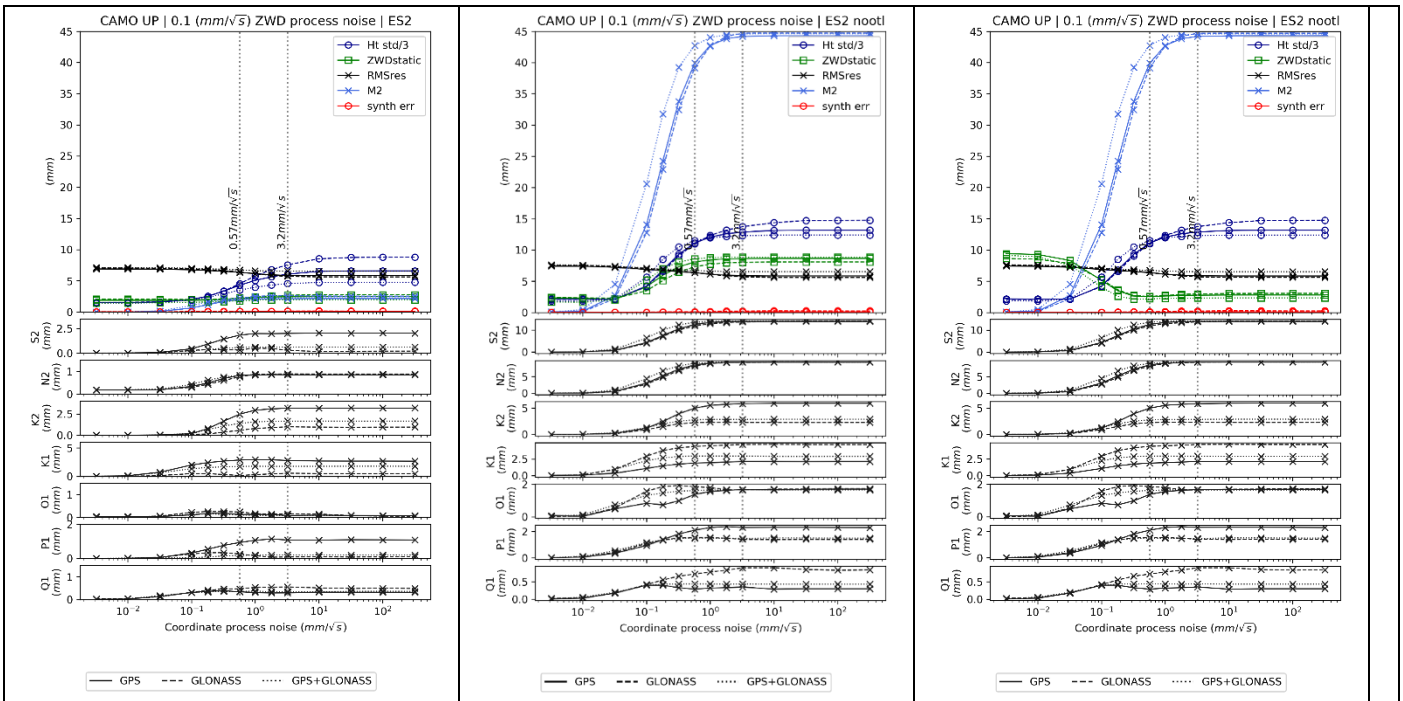

Figure R1. The effect of varying coordinate process noise at test site CAMO for the up component (2010.0 – 2014.0), performed with ESA repro2 products with OTL modelling enabled (left), disabled (centre and right) during PPP run. The right plot ZWDstatic was computed relative a static solution with OTL modelling enabled.

I think the estimated clocks and zenith troposphere also provide clues to this sensitivity problem. One could probe the time series of these “nuisance” parameters for signs of energy at the sidereal periods linked to the GPS repeats.
We tested the difference in estimated wet zenith delay between solutions with and without modelled OTL and found the difference to be negligible thus demonstrating that the zenith delay is not absorbing OTL with the chosen settings. The tropospheric gradients were also analysed, and the differences were again negligible. Given these and earlier tests by us and Penna et al. (2015) we are content that the solutions are optimal. To test if any tidal signal was absorbed by the wet zenith or gradient parameters, we repeated the solutions but without OTL modelled at the observation level and compared the sets of parameters. We found negligible differences suggesting that OTL is not being absorbed into these parameters without chosen process noise settings.

One other suggestion is to consider relegating additional detailed discussion to the supplementary material. The salient points sometimes get obscured by the detailed descriptions of the results and cases. The paper is otherwise well written.
We have reviewed the manuscript for overly detailed discussion of the results and editing the text appropriately throughout.

Response to Reviewer 2's remarks on "Estimating ocean tide loading displacements with GPS and GLONASS" se-2020-22

We thank the reviewer for meticulous review and constructive remarks that greatly impacted the quality of the prepared publication. We break down the points of the reviewer into sub blocks and respond in **bold.**

NOTE: On additional check we found some minor errors in our plotting routine which slightly affected figures 3, 6, 9, 10, 11 and their supplementary versions. We updated the figures and their analysis. These changes do not affect the conclusions.

The key updates are:

- **Fig 3: GPS AR (JPL) the variance in up is smaller by ~1.3 mm for S2 and 1 mm for K1 but larger by ~2.5 mm for K2**
- **Fig 6. CODE GPS a ~1 mm bias in S2 appears for solutions with cutoff angle >= 10 while median values change marginally.**
- **Fig 9. GPS (JPL) a ~0.7 mm bias in S2 east appears. The variances of K1 and K2 become smaller by ~2 mm**
- **Fig 10. GPS AR (JPL) shows a clearer linear dependency with cutoff angle.**
- **Fig 11. A constant ~0.3 mm S2 east bias appears**

1. Section 1 Introduction:
   1.1. It would be helpful to make clearer what the main aims and objectives of the paper are, in order to better put the many documented tests into context. The Introduction provides a generally useful overview of previous works and some limitations, but the last paragraph fails to build on this, just describing what will be included in the paper, without explaining why such tests are being done, or what the paper is seeking to achieve and why.
   The last paragraph of the Introduction was rewritten to clearly describe the tests and objectives. "We seek to improve estimates of OTL displacement from continuous GNSS data. especially for constituents that are subject to systematic error in GPS-only solutions (e.g., K1, K2, S2, P1) as found in previous studies (Allinson, 2004; King, 2006; Yuan & Chao, 2012)**. We do this by using both GLONASS and GPS data to estimate amplitudes and phases for the eight major OTL constituents (M2,S2,N2,K2,K1,O1,P1,Q1). Our work focuses particularly on understanding the sensitivity of estimates to different processing choices."**

   1.2. Please also revise some of the description about why anelasticity etc has not been studied until recently, as it is not the case (L41) that limitations in PREM were the reason. The limitations were the accuracy of the ocean tide models (as recognised on L47) and the quality and availability of GNSS measurements/processing.
   We revised this block to correct the limitations issue and better reflect the logical order of advancements. "This type of investigation has not been easily done previously due to various limiting factors such as the accuracy of ocean tide models and the quality and availability of GNSS observations. Accuracy advances achieved with recent altimeter-constrained ocean-tide models (Stammer et al., 2014) and evolving GNSS networks has enabled studies to identify limitations in the global seismic Preliminary Reference Earth Model (PREM) ..."
   The following paragraph was revised and appended to make this section more concise.

2. Section 2 Dataset selection:
   2.1. From Figure 1, one cannot see what M2 up OTL displacement the actual GNSS stations experience, except for those stations right on the coastline. This figure would be much more useful if the displacement over the land were also plotted.
   We updated the design of the Figure 1 with over-land OTL displacement.

   2.2. Note that the ocean tide model series is TPXO, so the model is TPXO7.2, not TPXO.7.2 (Figure 1 caption and L368).
   Corrected. Originally, we used naming as in free OTL provider.

   2.3. All stations in the figures and study are in Europe (L84), so please describe the stations' geographical distribution more accurately.
   The dataset description was updated to describe the locations: Of the 21 stations, 14 stations are in south-west England: covering both sides of Bristol channel (ANLX, SWAS, CARI, CAMO, PADT, APPL, TAUT) and northern coast of English Channel up to Herstmonceux (PMTH, PRAE, EXMO, PBIL, POOL, CHIO, SANO, HERT) with one site (BRST) in the south. Two sites are in northern England (WEAR, LOFT), two in Scotland (LERI, BRAE) with one site in central Europe (ZIM2). All sites are equipped with GPS+GLONASS receivers. Note that sites CAMO, LERI and ZIM2 sites replace CAMB, LERW and ZIMM respectively, that were used by Penna et al. (2015) because the earlier sites were replaced with newer ones, including adding GLONASS tracking.

   2.4. Regarding the selected stations, given that the GNSS minus model residual is being used as a quality indicator (with zero the aim), some indication of expected errors based on previous studies should be included.
   We have added a sentence which summarises the typical magnitude the differences between observations and models (~0.5-2mm depending on constituent and location) based on previous studies (e.g., Yuan et al., 2013).

   2.5. Are some of the larger residuals later shown likely to be associated ocean tide model or Green's function errors and hence not just indicators of GNSS measurement quality? E.g. Bos et al (2015) state that they excluded the GNSS stations CARI and SWAS from their geophysical results because of large ocean tide model discrepancies in the Bristol Channel.
   Here we assess the difference between various solutions using different products and constellation configurations , in terms of the effect on the residual OTL computed relative to some fixed modelled OTL. This means that the biases due to ocean tide

model or Green's functions are differenced. Thus, CARI and SWAS were not excluded.

3. Section 3 GNSS data processing:

   Please clarify what exact OTL model was used in the GipsyX processing and what was used in the subsequent results. It seems strange in a technical paper such as this where the variables are the GNSS constellations, orbits etc, to use some form of OTL model remove-restore procedure. Was hardisp used with FES2004 and Gutenberg-Bullen in the GipsyX processing? If so, I am not clear why it is then said on L140 that the "OTL displacements modelled in GipsyX were added back using HARDISP" when referring to the post-processed time series?

   We follow the procedure of Penna et al. (2015) here who in turn follow the work of King et al. (2000, 2003).As summarised in the response to reviewer #1, when we tested the alternative approach (e.g., comparison of techniques used by Penna et al. (2015) with those used by Martens et al. (2016)) we found differences of no more than 0.1mm (and this includes the effect of removing the companion tides so is a an upper bound). . We have amended the text at the first mention of FES2004 and GB to clarify that we later restore this signal.

   3.1. So if FES2004/Gutenberg-Bullen was used in the GipsyX processing, the carrier phase residuals shown in Figure 2 presumably contain some FES2004/Gutenberg-Bullen errors,

   This is not correct given we use a kinematic processing approach and hence mismodelled OTL is simply reflected in the time series. If the coordinate solution was 24hr rather than 5min, these data would affect the residuals.

   3.2. while the OTL up displacement also shown in Figure 2 is a residual to FES2014b/STW105d (how were these computed as, unlike for FES2004_GBe, there is no explicit statement of their source)?

   L110 updated to: All OTL values used in the publication were generated using CARGA software at the free ocean tide loading provider (http://holt.oso.chalmers.se/loading) (Bos & Baker, 2005).

   3.3. Hence are results from different OTL models displayed in the same figure, which would seem to be inconsistent?

   The residual displacement shown in Fig 2 is relative to FES2004_Gbe. This is mentioned on L173. We added "$\|Z_{res}\|$ is relative to FES2004_Gbe." to the figure caption.

   3.4. I do not follow the statement on L159-160 that FES2014b_STW105d is used unless stated otherwise, but then in Section 4, it is suggested that FES2004/Gutenberg-Bullen was used. Exactly what was used for which test needs to be clearly explained as it is hard to fully interpret the results at present, but why the need to mix and match?

   The M2 residual OTL values used in the test could be computed through analysis of raw timeseries. We, however, restore the OTL so need to subtract it to get the residual. If not restored, the phase STD values may be slightly distorted. We removed "computed by differencing observed OTL with FES2004_Gbe theoretical values ("M2")" to prevent confusion.
   L153 was updated to: "We then computed the vector difference between the *reconstructed observed* OTL and that predicted." to highlight the reconstructed full OTL signal used in further analysis.

   3.5. Please also note that CODE and ESA orbits provided via the IGS are in a centre of network (CN) frame, rather than CE. Regarding orbit and clock products, the authors should make clear that their statements regarding PPP AR and particular products are in the context of GipsyX, and not necessarily other GNSS processing softwares.

   While IGS orbits are in CN on a daily basis orbit products at sub-daily timescales are naturally in CM unless they are otherwise corrected for the CE-CM motion. The frame for sub-daily OTL is not dependent on a network of stations. CN is therefore not relevant to our study. We have added that "The findings in our paper are in the context of GipsyX software and solutions derived using other software may produce different results especially if the underlying model choices differ".

   3.6. On L136, please provide details as to what is meant by "The raw 4-yr timeseries were filtered".

   Changed to: Outliers were filtered from the raw 4-yr timeseries using two consecutive outlier-detection strategies: rejecting epochs with extreme clock bias values (>3x10^3 m) or where the XYZ σ was over 0.1 m; and then rejecting epochs with residuals to a linear trend larger than three standard deviations per coordinate component.

4. Section 4 Process noise optimization:

   4.1. Figure 2 shows that the M2 residual varies with the coordinate process noise, which is to be expected, yet the synthetic signal introduced (what amplitude?) is recovered with apparent zero error with all process noise ranges.

   see response to issue 4.2 and 4.3. Please note that the differences between our work and those of previous work are immaterial to the results and hence why this discussion is in the supplementary material.

   4.2. I think the authors need to carefully check their processing and implementation: there are various ways by which the effect of a synthetic signal can be introduced to GNSS processing, but intuitively if a very small coordinate process noise is applied, then one would not expect to be able to recover it.

   We clarify here that the synthetic signal is introduced as a nominal or a priori signal in GipsyX. As such, solutions with zero process noise, to take an extreme, are required to exactly follow the a priori since in this case no adjustment of the prior is allowed. That is, the solutions cannot deviate from the nominal. In that case, we regard the error should be zero (synth_err=0). The same situation effectively applies for very small (tight) process noise. We have now clarified in the text that this is the approach in GipsyX. We explain further under 4.3 the reason for the difference with previous studies.

4.3. Then in the supplement, the authors show that they recover a 6 mm amplitude synthetic signal perfectly with a very small process noise (which is counter-intuitive), but not at all with a larger process noise. Note that Martens et al (2016), which the authors cite but not in relation to synthetic signals, obtain results corroborating those of Penna et al (2015), in that the synthetic signal is not recovered if a very small process noise is applied.

We think this difference comes from either the use of an unintuitive (to us) definition of "error" in previous studies or from a misunderstanding in those studies of the output of a GIPSY routine. Our logic of how GipsyX works is outlined in 4.2 above. The opposite extreme is to have very high process noise in which case the solution adjusts away from the nominal to the solution governed by the data. In that case, the difference between the nominal and the solution should reflect the signal introduced in the nominal. We outline the problem in previous studies next: Let's take the smallest coordinate processing noise value on Fig 3 in Penna et al. (2015) which is 3.2 mm/sqrt(s). The synth_err parameter in their Figure 3 equals 6 mm, which essentially means that no synthetic signal was recovered given the synthetic signal was 6mm. If we repeat this test and then convert the XYZ coordinate solutions from the GIPSY output data file (tdptable) to ENU using the GIPSY xyz2env/xyz2llh script, (tdp2envDiff.py GipsyX) we find a value of synth_err of 0 mm not 6mm. However, if we plot the XYZ coordinate components from the output tdptable directly, they show the clear synthetic signal that we introduced. How is this possible? The answer lies in the xyz2env script which differences XYZ values (column 2 of the tdpfile) with their nominals (column 1 of the tdpfile) before rotation. We know that our timeseries with that tight noise will perfectly resemble the nominals we introduced (synth signal), so if we difference it with the nominals we get a straight line – cancelling out the signal and producing an apparent time series that is a straight line and hence, when differenced from the original signal, produces a 6 mm synth_err . We resolved this by creating a custom xyz2env script and we get the expected results – inverted dependency. As we note above, the points in 4.1, 4.2, 4.3 have no direct bearing on the conclusions of our work or previous work.

added "We only present results without a synthetic signal introduced into the sites' nominal location, with further discussion in the supplementary material (Fig. S6)."
removed "The only difference in our results to those of Penna et al. (2015) were for the "synth err" test, where our results are inverted (but without changing the magnitude); the reason for this is discussed in detail in the supplementary material."

4.4. The authors also state in the supplement that in kinematic positioning constant nominal coordinates should be used, but this is not always appropriate, for example the case of a rapidly moving GNSS receiver.

We do not consider rapidly moving GNSS receivers and cannot conceive of a case where OTL studies would use such a receiver. As such we do not make any changes to the text.

5. Section 5 and Section 5.1:

5.1. Overall, I found the order and logic of all these tests a bit piecemeal and not particularly well flowing and ordered. To improve the readability, I encourage the authors to improve the description of why each test was undertaken, and how they build on the preceding ones.

We added to the end of introductory section (5): We now explore the sensitivity of our solutions to different products and analysis choices starting with elevation cutoff angle sensitivity, directly related to the amount of possible multipath presence. We follow with intercomparison of various products solutions and assessing impact from integer ambiguity resolution (GPS only) to understand the possible associated inconsistencies. Finally, we test fidelity of Eterna software to various constituents and timeseries length.
We have also added a single sentence to the beginning of each test to explain how each test flows from the previous.

5.2. Section 5.1, although entitled "Effect of using GLONASS", is really a generic introduction to the subsequent tests, as almost all of them assess the effects of GLONASS and GPS+GLONASS in some way. So I think this section would be better as an introductory Section 5, that then leads into the others. For example, it seems odd to include so little discussion in Section 5.1 on the benefits of using GLONASS for K2 and K1, and the overall performance of GLONASS and GPS+GLONASS. I was left wondering where this was given the section heading, until I saw a separate section called "K2 and K1 constituents".

We updated 5.1 to a more general 5

5.3. Please include quantification in the description of improvements, rather than simply saying, for example, "smaller". Any suggestions as to why there are variations in residuals among the different constellations and ambiguity fixing approach for the different coordinate components?

The paragraph was revised to reflect the updated Fig. 6 and to quantify the estimates. While we want to only highlight the differences within multiple parameters that have great effect on OTL estimates, several factors such as satellite's orbit models and different handling of inter-frequency & inter-system biases (GLONASS) are of higher importance. Also, the period analysed here is the worst in terms of GLONASS availability as the constellation was only fully restored (24 SVs) in March 2010. The note on constellation restoration information was added.

6. Section 5.3: It seems strange that the complete opposite of larger vs smaller GPS or GLONASS residuals arises when using CODE and ESA orbits and clocks. Any more explanation for this? For instance, I am not clear why the correction of atmospheric tides in the CODE products will improve GPS but not GLONASS?

We suggest it can only come from satellite orbit modelling differences propagating to orbit and clocks errors and/or multipath, although the exact source is not clear to us and would require a substantial study focused on product generation. We have removed mention of atmospheric tides as, we agree, it cannot affect GPS and GLONASS differently.

7. Section 5.6 Noise and uncertainty:
   7.1. This paper concerns the generation and analysis of OTL displacement residuals. So if the modelled OTL displacements applied are in a frame compatible with the orbital products, as I assume has been done throughout the paper (this is implied on L106-107), then are the residuals (and their uncertainties) actually sensitive to the frame given the model and GNSS measurement precisions? Figures 3-5, in which JPL and CODE/ESA residuals are compared, do not suggest the residuals themselves are.
   Our assumption is that inconsistencies between frames are far too small to be noticeable. Additional testing (purely synthetic) suggests the possible presence of minor inconsistencies between CoM coefficients computed with FES2004 and FES2014b ocean tide models. However, they are concentrated within K1 and O1 constituents with magnitudes of ~0.2 mm in each component. This suggests that frame inconsistencies should be considered in the future, especially with MultiGNSS AR processing by correcting for residual CoM in CE solution due to limitations of FES2004 used according to IERS recommendations. This is a subtle detail that is not core to the paper and so we do not further extend the paper by adding a discussion.

   7.2. It is not clear how the JPL products in CM "provide a significant advantage" (L288) over ESA and CODE products in **CE (CN)** in relation to phase uncertainties. The authors state that the effect will depend on the constituent's amplitude, but the CE-CM difference (and hence whether the CM value or CE value has the larger amplitude) will depend on the location globally. What exactly has been applied in the creation of the two panes in Figure 8?
   Our remarks pertain to the study region. We took the standard deviation values of phase measurements returned by Eterna and averaged them per component and constituent. We added a short note to Fig. 8 caption.

   7.3. I am also puzzled by the results for the averaging of the amplitude uncertainties across all constituents. It seems odd that the K1 and K2 amplitude uncertainties are commensurate in precision with the lunar constituents such as M2 and N2, given the errors and associated problems with K1 and K2.
   The results were checked and confirmed suggesting that Eterna is not facing any limits related to the constituent.

8. Section 5.8 Timeseries length:
   8.1. The authors should summarise the status of the various IGS Analysis Centre reprocessing and operational products for the reader who might not have intricate knowledge of what was done and when, and hence what timespan such products cover. What are the key differences between the repro2 products of 2010.0-2014.0 and those used for 2014.0-2019.0?
   The goal of reprocessing campaign was to preserve consistency with operational products (Griffiths, 2019)**, thus we assume the differences to be insignificant and not impacting the estimates. Text updated.**

   8.2. If the operational products adopted repro2 procedures for much of this time, then one would not expect noticeable changes, but if major changes arose in the operational products during the 5 year window, then comparing time series lengths involves multiple variables, when the desire is to just vary the time series length. To me it would be better to describe the test shown in Figure 12 first, in order to evaluate the impact of any differences in products, as well as showing another test of measurement noise.
   We swapped figures 11 and 12 according to your recommendation.

   8.3. The authors say they found no significant differences at M2, N2, O1, P1 and Q1, but Figure 12 suggests there is a noticeable difference at P1 for GPS, perhaps unsurprisingly given P1 challenges discussed earlier in the paper.
   Based on previous results, we assumed that changing satellite orbit and clock products may produce substantial differences in problematic solar-related constituents (S2, K2, K1, P1). We better describe the repro/operational products test.

   8.4. It is stated on L335-336 that GLONASS showed significant differences for K1 and K2, but Figure 12 suggests the differences are bigger for GPS, so what is implied here? It is stated on L325 that all eight constituents' variation with time series length was assessed, but then only S2 and K1 are shown (in Figure 11) and discussed. I had to search through the supplement to find the other constituents, but this needs to be made clear in the paper itself, and state why the emphasis in the paper is on S2 and K1.
   The text has been updated to make the implication clearer that focus on S2 up is due to the evolution of inverted $\|Z_{res}\|$ bias and K1 up, as most problematic diurnal constituents.

   8.5. Many of the constituents appear (from inspection of the supplement) stable over time, which suggests that even if there are changes in the products, they are not having an impact. I think more should be made of this point in this section, as it is a positive result.
   We added this point. If constituents selected according to optimum constellation strategy, $\|Z_{res}\|$ appear (see Fig. S4) stable over time, which suggests that even if there are changes in the products, they are not having an impact with this methodology.

   8.6. I am unclear what is meant by the sentence on L338-339 – please rewrite.
   We completely reviewed this section to improve the description of the products.

9. Supplement: It is not clear what new information related to tidal cusps has been found by the authors or why they have raised this point. Section 6.1.1 of the Penna et al (2015) study does not state that there are tidal cusps, but discusses that any slight gradual increases in power around M2 are likely caused by spectral leakage.
   We removed the sentence which mentioned tidal cusps as it is indeed irrelevant.

10. Other points:

10.1. Please provide a concise statement defining the bounds of the box and whisker plots used throughout the paper, as there can be different conventions used. E.g. on L191 I did not follow what is meant as the stated lower bound.
We remove "(25th percentile - 1.5*interquartile range), which is present at all sites no matter how far inland."
Added at L159: "We utilize box-and-whisker plots to demonstrate the distribution of the estimates with the boxes defined by the interquartile range (IQR), with median as a horizontal line, and whiskers by an additional +- 1.5 * IRQ.

10.2. Please decide on "vector difference" or "vector distance", and use consistently throughout the paper.
All instances of "vector distance" were changed to "vector difference"

10.3. L58: Not clear why ESA and CODE orbit/clock products are specifically mentioned here but those from other IGS Analysis Centres are not. The justification for these two is provided in Section 3, but on L58 the mentions are out of place and premature without more explanation.
This early mention of ESA and CODE products "*(ESA, but not CODE)*" was removed so not to confuse the reader.

10.4. L203: Please explain in what way different elevation cut-off angles will modulate the expression of signal multipath into solutions. I think you mean by this that you expect less multipath with larger cut-offs?
we updated L203: "Different elevation cutoffs will significantly alter the observation geometry as well as modulate the expression of signal multipath into solutions, decreasing its amount with higher cutoff value."

10.5. L209-210: What is meant by the sentence "For the. . . (including K1 and K2)"? It does not make sense, and what does increase the stability mean?
Stability means closeness of estimates between solutions (e.g. different cutoff angles). Part of the paragraph was updated to eliminate confusion and explicitly highlight the stability term.
We updated the sentence to "GPS+GLONASS shows smallest $\|\Delta Z_{res}\|$ between 7° and 20° estimates for S2 and P1 (0.31, 0.23 mm, respectively) and an additional decrease in $\|\Delta Z_{res}\|$ for M2, S2, N2, O1, Q1 in the up component, which indicate higher closeness of compared OTL values – higher stability with changing cutoff angle."

10.6. L211-213: Sentence contradicts itself. Please clarify.
L211-L213 updated to: The same comparison done for GPS AR (7° and 20° cutoff, JPL native products) shows largely improved stability in comparison to all GPS only ambiguity free solutions (Figure 4, bottom).

10.7. L221-222: By "partial expression", do you mean partially propagate?
Yes. Changed "...all satellite-related systematic errors will partially propagate into station-specific parameters"

10.8. L253-255: Please refer to Figure 3 so that the reader can ascertain what is being referred to.
Updated to : "As seen from Fig. 3, ...". In addition, removed Δ from $\|\Delta Z_{res}\|$, as Fig. 3 shows $\|Z_{res}\|$.

10.9. L256: Is 'tightest' a technical term?
term tightest was changed to "*have lowest variance*". Text was updated accordingly.

10.10. L258-259: What is meant by "The GLONASS K1 east is not true"?
The paragraph was updated

10.11. L270-271: What is meant by "better consistency between products"? I think it better to say that GLONASS gives smaller values, rather than being "preferred".
As suggested by the reviewer, we reviewed the sentence: "GLONASS returns smaller $\|Z_{res}\|$ in the K2 and K1 north and up components while east component might show better results with GPS+GLONASS (K1, CODE) but, due to higher closeness between products, GLONASS constellation is still preferred."
We leave preferred in the end as this applies to the optimum constellation configuration.

10.12. L313-314: Please state where (this paper?) the "similar behaviour previously observed with ESA products" was.
Added (Fig. 6)

10.13. L315-316: Please refer to the figure in question, and quantify "completely" and "slight increase". L316: It is mentioned that the implementation of ambiguity resolution results in a slight increase in the median of the up component. Any explanation for this? From inspection of Figure 10, I am not convinced anything of significance is showing compared with the float solutions.
We updated the paragraph: "Enabling integer ambiguity resolution (GPS AR) removes the ~1 mm S2 $\|Z_{res}\|$ bias completely at 7° and 10° elevation cutoff angles while leaving ~0.4 mm bias at 15° and 20° in the up component. Consequently, up $\|Z_{res}\|$ medians decrease by 1-2 mm depending on elevation cutoff angle. Based on this observation, we expect that utilising ambiguity resolution within PPP might help in solving, or at least minimising, the S2 $\|Z_{res}\|$ present in ESA GPS and CODE GLONASS solutions. Eliminating biases in GPS and GLONASS separately should increase the stability and consistency of GPS+GLONASS S2 $\|Z_{res}\|$."

The authors need to carefully go over the English and presentation to improve the readability of the paper (particular the use of "the") and ensure all acronyms and abbreviations are defined. Non-exclusive examples (in Sections 1-3 only) include:
L3: "close to several" -> "close to that of several" ***Corrected***
L4: is -> are ***Corrected***
L5: over -> of ***Corrected***
L6: "Western Europe" -> "western Europe" ***Corrected***
L17: hyphen not needed in "solid Earth" ***Corrected***
L24: Incorrect reference format ***Corrected***
L31 (and elsewhere): The reference should be Wang et al (2020) not 2019. L451-453 is out of date ***Corrected***
L33: I would put "predominantly" before "estimated" ***Corrected***

L49: “areas”, rather than “conditions”? **We might stick with conditions as in Stammer**
L54: I would add “period” and “orbital” **Not clear here**
L55: “constellation period” -> “constellation repeat period” ***Corrected***
L62: “constellation period” -> “constellation repeat period” ***Corrected***
L62: remove spaces before the “11” and “8” ***Corrected*** **with tilde changed to $\sim$. Same with L79**
L79: “observation” -> “observations” ***Corrected***
L80: insert “the” before “selected” ***Corrected***
L105: change to “within each processing” ***Corrected***
L107: No need to describe the file format**. simplified to “The OTL values were generated using CARGA software at the free ocean tide loading provider (http://holt.oso.chalmers.se/loading) (Bos and Baker, 2005).”**
L108: change to “using the free” ***Corrected (see above)***
L110: change “single products solution” to “single product’s solution” ***Corrected***
L113: change “Products” to “products” ***Corrected***
L134: no need to describe the basic merging / concatenation of IGS files ***Corrected:*** **Removed “…and merging the IGS-standard 24-h orbits/clocks into 30-h where necessary”**
L143: insert “the” before “processing” ***Corrected***
L146: insert “the” before “Eterna” ***Corrected (check with Matt)***
L148: remove “the” before “solid Earth” ***Corrected***
L151: remove “using the procedure” ***Corrected***
L158: first bracket is in the wrong place ***Corrected***

We additionally reviewed the manuscript from section 4 onwards for minor issues as suggested by the reviewer

Estimating ocean tide loading displacements with GPS and GLONASS

Bogdan Matviichuk[1], Matt King[1], and Christopher Watson[1]

[1]School of Technology, Environments and Design, University of Tasmania, Hobart, 7001, Australia

Correspondence: Bogdan Matviichuk (bogdan.matviichuk@utas.edu.au)

Abstract. Ground displacements due to ocean tide loading have previously been successfully observed using GPS data, and such estimates for the principal lunar M_2 constituent have been used to infer the rheology and structure of the asthenosphere. The GPS orbital repeat period is close to that of several other major tidal constituents (K_1, K_2, S_2) thus GPS-estimates of ground displacement at these frequencies ~~is~~ are subject to GPS systematic errors. We assess the addition of GLONASS to increase the accuracy and reliability ~~over~~ of eight major ocean tide loading constituents: four semi-diurnal (M_2, S_2, N_2, K_2) and four diurnal constituents (K_1, O_1, P_1, Q_1). We revisit a previous GPS study, focusing on 21 sites in the UK and ~~Western~~ western Europe, expanding it with an assessment of GLONASS and GPS+GLONASS estimates. In the region, both GPS and GLONASS data are abundant since 2010.0. We therefore focus on the period 2010.0-2014.0~~which is~~ , a span considered long enough to reliably estimate the major constituents. Data were processed with a kinematic PPP strategy to produce site coordinate time series for each of 3 different modes: GPS, GLONASS and GPS+GLONASS. The GPS solution with ambiguities resolved was used as a baseline for performance assessment of the additional modes. GPS+GLONASS shows very close agreement with ambiguity resolved GPS for lunar constituents (M_2, N_2, O_1, Q_1) but with substantial differences for solar-related constituents (S_2, K_2, K_1, P_1), with solutions including GLONASS being generally closer to model estimates. While no single constellation mode performs best for all constituents and components, we propose to use a combination of constellation modes to recover tidal parameters: GPS+GLONASS for most constituents except for K_2 and K_1 where GLONASS (north and up) and GPS with ambiguities resolved (east), perform best.

1 Introduction

Earth's gravitational interactions with the Sun and the Moon generate ~~solid Earth~~ solid Earth and ocean tides. These tides produce periodic variations in both the gravity field and Earth's surface displacement. Additionally, the ocean tides produce a secondary deformational effect due to associated periodic water mass redistribution, known as Ocean Tide Loading (OTL) (e.g., Agnew, 2015; Jentzsch, 1997; Baker, 1984). OTL is observable in surface displacements (and their spatial gradients, i.e. tilt and strain) and gravity. Displacement and gravity attenuate approximately as the inverse of the distance from the point load while gradients have this relation but with distance squared (Baker, 1984). Thus, OTL displacement and gravity changes show greater sensitivity to regional solid Earth structure in comparison to tilt or strain observations ~~Martens et al. (2016)~~ (Martens et al., 2016), making this an observation of interest for studying solid Earth rheology.

Global Navigation Satellite Systems (GNSS) are particularly convenient for measuring OTL displacements due to the widescale deployment of dense instrument arrays. Data from continuous GNSS stations have been shown to provide estimates of OTL with sub-millimetre precision using two main approaches as described by Penna et al. (2015): the harmonic parameter estimation approach – OTL displacement parameters are solved for within a static GNSS solution (e.g., Schenewerk et al., 2001; Allinson, 2004; King et al., 2005; Thomas et al., 2006; Yuan and Chao, 2012; Yuan et al., 2013); and the kinematic approach – OTL constituents are predominantly estimated from high-rate kinematic GNSS-derived time series ~~(e.g., Khan and Tscherning, 2001; King and Aoki, 2003; King, 2006; Penna et al., 2015; Martens et al., 2016; Wang et al., 2020)~~ (e.g., Khan and Tscherning, 2001; King, 2006; Penna et al., 2015; Martens et al., 2016; Wang et al., 2020). In this paper, we follow the kinematic approach.

To date, GNSS-derived OTL displacements have been estimated using predominantly the US Global Positioning System (GPS). GPS-derived measurements of Earth-surface displacement at tidal periods have been successfully used to observe OTL displacement and validate ocean tide models (Urschl et al., 2005; King et al., 2005). The residual displacement between observed and predicted OTL has been related to deficiencies in ocean tide models, reference-frame inconsistencies, Earth model inaccuracies, the unmodelled constituents' dissipation effect and systematic errors in GPS (e.g., Thomas et al., 2006; Ito and Simons, 2011; Yuan et al., 2013; Bos et al., 2015).

Recent studies have made use of GPS-derived OTL to study dissipation or anelastic dispersion effects in the shallow asthenosphere at the M_2 frequency (e.g. Bos et al., 2015). This type of investigation has not been easily done previously due to various limiting factors ~~. One key limitation was the limitations of the~~ such as the accuracy of ocean tide models and the quality and availability of GPS observations. Recently, however, models have improved dramatically with the use of satellite altimetry (Stammer et al., 2014), and GNSS networks have both expanded and have improved data quality. Together, this has enabled the exploration of limitations in the global seismic Preliminary Reference Earth Model (PREM) (Dziewonski and Anderson, 1981) ~~that were demonstrated~~ with GPS observations in the western United States (Ito and Simons, 2011; Yuan and Chao, 2012), western Europe (Bos et al., 2015), South America (Martens et al., 2016), Eastern China Sea region (Wang et al., 2020) and globally (Yuan et al., 2013). These limitations are associated partially with the incompatibility of the elastic parameters within the seismic (1 s period) and the tidal frequency bands and the anelasticity of the upper layers of the Earth, particularly the asthenosphere~~(Wang et al., 2020).~~

~~The use of OTL to probe the asthenosphere is increasingly possible because of accuracy advances of the global ocean tide models over recent time. Comparison of seven recent altimeter-constrained ocean-tide models to tide gauge and bottom pressure data shows agreement for eight major constituents of 0.9, 5.1 and 6.5 cm for pelagic, shelf and coastal conditions respectively (Stammer et al., 2014). Bos et al. (2015) used this accuracy to infer that GPS-derived OTL displacement estimates were different to modeled displacements due to asthenospheric anelasticity. Lau et al. (2017) used results~~ . The latter was studied through modelling the GPS-observed residuals of the major lunar tidal constituent, M_2, by Bos et al. (2015) and, later, Wang et al. (2020), while Lau et al. (2017) used M_2 residual from the global study of Yuan et al. (2013) to constrain Earth's deep-mantle buoyancy.

Previous studies have highlighted an apparently large error in solar-related constituents estimated from GPS, in particular K_2 and K_1. This is in part due to their closeness to the GPS orbital (K_2) and constellation (K_1) repeat periods, which strongly aliases with orbital errors. The closeness to the GPS constellation repeat period may induce interference from other signals such as site multipath which will repeat with this same characteristic period (Schenewerk et al., 2001; Urschl et al., 2005; Thomas et al., 2006). Additionally, the P_1 constituent has a period close to that of 24 hours which is the timespan used for the IGS-standard orbit and clock products ~~(ESA, but not CODE)~~ (Griffiths and Ray, 2009), and hence may be contaminated by day-to-day discontinuities present in the products (Ito and Simons, 2011).

Urschl et al. (2005) proposed that the addition of GLONASS (GLObal NAvigation Satellite System), a GNSS developed and maintained by Russia (USSR before 1991), could improve the extraction of K_2 and K_1 constituents as the orbit period of the GLONASS satellites (~~~~11 h 15 min 44 sec) and constellation ~~period (~~ repeat period (~~~~8 days) are well separated from major tidal frequencies. However, for many years GLONASS suffered from an unstable satellite constellation and very sparse network of continuous observing stations. This has been progressively addressed over the last decade to the point where many national networks now include a high density of GLONASS (and other GNSS) receivers.

~~In this publication, we expand the methodology described in Penna et al. (2015) with two more constellation configurations: stand-alone~~ We seek to improve estimates of OTL displacement from continuous GNSS data, especially for constituents that are subject to systematic error in GPS-only solutions (e.g. S_2, K_2, K_1, P_1) as found in previous studies (Allinson, 2004; King, 2006; Yuan and C . We do this by using both GLONASS and GPS ~~+GLONASS; we also increase the number of assessed constituents to eight:~~ data to estimate amplitudes and phases for the eight major OTL constituents (M_2, S_2, N_2, K_2, K_1, O_1, P_1, Q_1). As in the very recent study of Abbaszadeh et al. (2020), our work focuses particularly on understanding the sensitivity of estimates to different processing choices, although our work focuses on quite dense network in western Europe while their work focused on a globally-distributed set of stations. ~~The dataset used in this study is completely overlayed by the original study dataset thus enabling a crosscheck between published GPS results. Afterwards, we intercompare the OTL estimates from GPS, GLONASS and a combined GPS+GLONASS solutions acquired with different orbit and clock products in order to assess the constituent-specific sensitivities towards constellation/products configurations.~~

2 Dataset

~~Penna et al. (2015) validated GPS-derived estimates of OTL for geophysical interpretation while Bos et al. (2015) followed the previous study to analyse OTL displacements in western Europe . As previously stated, to quality control our analysis we decided to follow the validation approach and study region of Penna et al. (2015), but extended it to include GLONASS and GPS~~The sites used in our study are shown in Figure 1, with a focus on south-west England where a large M_2 OTL signal is present. Of the 21 stations, 14 stations are in south-west England: covering both sides of Bristol channel (ANLX, SWAS, CARI, CAMO, PADT, APPL, TAUT) and northern coast of English Channel up to Herstmonceux (PMTH, PRAE, EXMO, PBIL, POOL, CHIO, SANO, HERT) with one site (BRST) in the south. Two sites are in northern England (WEAR, LOFT), two in Scotland (LERI, BRAE) with one site in central Europe (ZIM2). All sites are equipped with GPS+~~GLONASS solutions.~~

GLONASS receivers. Note that sites CAMO, LERI and ZIM2 sites replace CAMB, LERW and ZIMM respectively, which were used by Penna et al. (2015), to allow for use of GLONASS data recorded at the former set of sites.

Aside from the addition of GLONASS data, an important difference to the ~~original studies~~ study of Penna et al. (2015) is the shift in time period from 2007.0–2013.0 to 2010.0–2014.0. This shift provides sufficient GLONASS data following the upgrade of many receivers to track ~~GNSS from 2009.~~ GLONASS from 2009 that followed the restoration of the GLONASS constellation finished in March 2010 (24 SVs). Despite this covering a shorter time span, the length of continuous ~~observation within~~ observations at each site (minimum availability of ~~0.95 through~~ 95% through the dataset) exceeds the recommended ~~~~1000 days of continuous observations (4 years with ~~0.7~~ 70% availability) (Penna et al., 2015). ~~Additionally,~~ The selected time period is fully covered by a complete and homogeneous set of reprocessed orbit and clock products.

The ~~sites used in our study are shown in Figure 1, with a focus on south-west England where a large M_2 OTL signal is present. Of the 21 stations, 14 stations are in south-west England and the southern part of Wales with an additional seven stations in Europe, all equipped with GPS+GLONASS receivers. Our station set is somewhat different to that used by Penna et al. (2015) due to the lack of GLONASS-capable receivers, replacement with sites a few metres away, or the addition of new sites which were deployed just before 2010.0.~~

~~The~~ chosen sites experience a range of M_2 up OTL amplitudes~~ranging~~ , from > 30 mm (ANLX, APPL, BRST, CAMO, PADT, PRAE), 15-30 mm (CARI, EXMO, LOFT, PBIL, SWAS, TAUT) and < 15 mm (BRAE, CHIO, LERI, POOL, SANO, WEAR, ZIM2). ~~Because of the wide range of experienced OTL within the dataset, a detailed sensitivity assessment of constituent/constellation configurations pairs became possible.~~

3 GNSS data processing strategy

The processing strategy was largely based on the GPS-only kinematic Precise Point Positioning (PPP) approach (Zumberge et al., 1997) as per Penna et al. (2015), but with important modifications in terms of the software and to permit the inclusion of GLONASS data. We address PPP in three different modes here: GPS, GLONASS and combined GPS+GLONASS. In particular, we use NASA JPL's GipsyX (~~v. 1.3~~v1.3), which is a substantial rewrite of the now legacy GIPSY-OASIS code to allow for, amongst other things, multi-GNSS analysis. Penna et al. (2015) used GIPSY-OASIS v6.1.2. We adopted a PPP solution approach and estimated station positions every 5 minutes with a random walk model introducing estimated optimum between-epoch constraints on coordinate evolution. We used the VMF1 gridded troposphere mapping function, based on the European Centre for Medium-Range Weather Forecasts (ECMWF) numerical weather model (Boehm et al., 2006). Additionally, ECMWF values for the hydrostatic zenith delay and wet zenith delay were used as a priori values for stochastic estimation of the wet zenith delay as a random walk process with optimum process noise values (Sect. 4) and tropospheric gradients were estimated as a random walk process (Bar-Sever et al., 1998), with process noise at 0.005 mm/sqrt(s). An elevation cut-off angle of seven degrees was applied, sufficient to maximize the number of GLONASS observations at the respective site latitude as noted by Abbaszadeh et al. (2020), together with observation weights that were a function of the square-root of the sine of the satellite elevation angle.

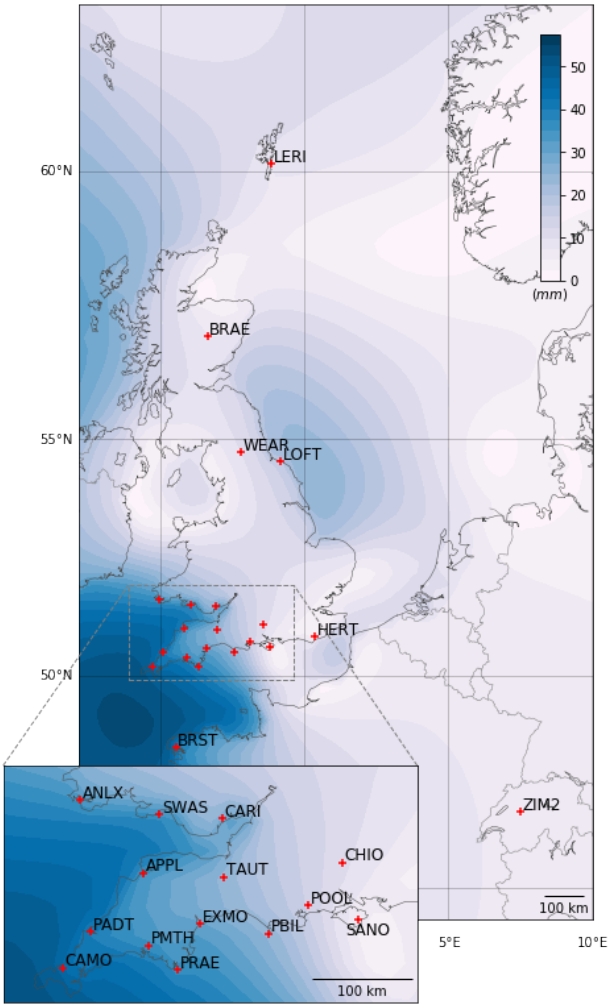

Figure 1. Map of the study area with GNSS site codes and M_2 up displacement amplitude in the background (~~TPXO.7~~TPXO7.2 ocean tide model and spherically symmetric earth with PREM structure).

Earth body-tide (EBT) and pole tides were modelled according to IERS 2010 Conventions (Petit and Luzum, 2010). The OTL displacement within each processing run was modelled with the FES2004 tidal atlas (Lyard et al., 2006) and elastic Green's functions based on the Gutenberg-Bullen Earth model (Farrell, 1972) (referred to as FES2004_GBe), with centre-of-mass correction applied depending on the adopted orbit products. The FES2004-based OTL values were ~~generated in BLQ format for 11 principal constituents (M_2, S_2, N_2, K_2, K_1, O_1, P_1, Q_1, Mf, Mm and Ssa) using~~ computed using the free ocean tide loading provider that uses OLFG/OLMP software (http://holt.oso.chalmers.se/loading) ~~.~~ while the rest of OTL values used in this publication were computed with CARGA software (Bos and Baker, 2005). We did not model atmospheric S_2 tidal displacements.

PPP requires pre-computed precise satellite orbit and clock products for each constellation processed which should be solved for simultaneously within a single ~~products~~ product's solution. Unfortunately, JPL's native clock and orbit products are not yet available for non-GPS constellations hence we adopted products from two International GNSS Service (IGS) (Johnston et al., 2017) Analysis Centres (ACs): the European Space Agency (ESA) and Centre for Orbit Determination in Europe (CODE). The ESA combined GPS+GLONASS ~~Products~~ products from the IGS second reprocessing campaign (repro2) were used (Griffiths, 2019) while CODE's more recent REPRO_2015 campaign (Susnik et al., 2016) had to be used as CODE's repro2 are lacking separate 5 min ~~clock corrections~~GLONASS clocks.

All three products consist of satellite orbits and ~~satellite clock corrections~~clocks, sampled at 15 and 5 minutes respectively, that were held fixed during our processing. The benefit of using JPL's native products, even though solely GPS, is the ability to ~~do~~ perform PPP processing with integer ambiguity resolution (AR). PPP AR in GIPSY-OASIS/GipsyX software packages can be performed by using wide lane and phase bias tables which are part of JPL's native products (Bertiger et al., 2010). To provide comparison with previous studies, GPS was processed with JPL's native orbit and clock products from the repro2 campaign (JPL's internal name is repro2.1) with AR.

The CODE and ESA clock and orbit products were generated in different ways. CODE's REPRO_2015 orbit positions were computed using a 3-day data arc, while ESA used a 24-h data arc (Griffiths, 2019). Both ACs provided orbits in a terrestrial reference frame, namely IGS08 and IGb08, respectively, that are corrected for the centre of mass (geocentre) motion associated with OTL (FES2004 centre of mass correction) and are in the CE frame, following ~~Blewitt (2003)~~Fu et al. (2012). Alternatively, JPL products were generated from a 30-h data arc, and were computed with stations in a near-instantaneous frame realisation hence the orbits are in the CM frame (we note that the JPL products distributed by the IGS are, by contrast, in CE). Considering the above, the modelled OTL values for JPL's native products solutions were corrected for the effect of geocentre motion while ESA/CODE products do not require this correction (Kouba, 2009).

It has been suggested that orbit arc length for a given product could potentially impact the estimated OTL displacements. In particular, Ito and Simons (2011) suggest that a 24-h data arc length (as per ESA products) may affect the P_1 constituent due to similarity of the periods. This is in addition to day-boundary edge effects given analysis of data in 24-h batches. We mitigate these effects to some extent by processing the ground stations in 30-h batches (allowing 3-h either side of the nominal 24-h day boundary)~~and merging the IGS-standard 24-h orbits/clocks into 30-h where necessary~~.

We post-processed the estimated coordinate time series as per Penna et al. (2015): the resulting 5-min sampled solutions were clipped to the respective 24-h window and merged together. ~~The~~ Outliers were filtered from the raw 4-yr timeseries ~~were filtered,~~ using two consecutive outlier-detection strategies: rejecting epochs with extreme receiver clock bias values ($> 3 \times 10^3$ m) or where the XYZ σ was over 0.1 m; and then rejecting epochs with residuals to a linear trend larger than three standard deviations per coordinate component. The XYZ timeseries were converted to a local east-north-up coordinate frame, detrended and resampled to 30-min sampling rate via a simple 7-point window average (7 samples -> 1 sample). 30-min averaging reduces high frequency noise (unrelated to OTL) as well as the computational burden of further harmonic analysis.

Finally, OTL displacements modelled in GipsyX were added back using HARDISP (Petit and Luzum, 2010). HARDISP uses spline interpolation of the tidal admittance of 11 major constituents to infer values of 342 tidal constituents and generate a

time series of tidal displacements. This approach almost eliminates the effect of companion constituents (Foreman and Henry, 1989) as they are modelled during ~~processing stage, even considering errors present in companion constituent displacement as tide model errors become neglectable for constituents this small~~the processing stage; small errors in the modelled major OTL constituents will propagate into negligible errors in modelled companion tides. Thus, the analysed harmonic displacement parameters represent true displacement plus an indiscernible companion constituent error ~~, far below~~ that is far below the measurement error. The findings in our paper are provided in the context of GipsyX software and solutions derived using other software may produce different results especially if the underlying model choices differ.

The harmonic analysis of the reconstructed OTL signal was performed using the Eterna software v.3.30 (Wenzel, 1996)~~with a high-pass filter (30-min sampling)~~, resulting in amplitudes and local tidal potential phase lags negative which are suitable for ~~the~~ solid Earth tide studies. OTL phase-lag, however, is defined with respect to the Greenwich meridian and phase lags ~~positive.~~

~~The latter, however, is not important for the purposes of this publication as we ignore the long-period tides in the analysis but used them for internal Eterna testing; same goes for diurnal tides phase rotation as all sites' latitudes are positive~~here~~are positive~~. Transforming to Greenwich-relative lags was done ~~using the procedure~~ according to Boy et al. (2003) and Bos (2000).

We then computed the vector difference between the ~~observed OTL vector~~ reconstructed observed OTL and that predicted by the model, following the notation of Yuan et al. (2013):

$$Z_{res} = Z_{obs} - Z_{th} \tag{1}$$

In Eq. 1 we assume body tide errors to be negligible, thus Z_{obs} is simply an observed OTL and Z_{th} is a theoretical OTL ~~. Residual OTL,~~ while Z_{res}, ~~is the difference between OTL model predictions and observational errors. The residual OTL~~the residual OTL, is their vector difference. Z_{res} presented in this ~~paper~~ publication is, if not otherwise specified, relative to the theoretical OTL values computed using the FES2014b ocean tide atlas, a successor of FES2012 used in ~~(Bos et al., 2015)~~ Bos et al. (2015), and a Green's function based on the STW105 Earth model additionally corrected for dissipation at the M_2 frequency which we call STW105d (referred to as FES2014b_STW105d). We utilize box-and-whisker plots to visualise the distribution of the estimates with the box and whiskers defined as the inter-quartile range (IQR) and an additional $\pm 1.5 \times$IQR, respectively, with the median as a horizontal line.

4 Process noise optimization

Process noise settings within GipsyX need to be chosen to ensure optimal separation of site displacement, tropospheric zenith delays, noise etc. For example, a tight coordinate process noise value, even the default value of 0.57 mm/sqrt(s), ~~tend~~ tends to clip OTL amplitudes, especially in ~~costal~~ coastal sites. Penna et al. (2015) developed a method of tuning process noise values for GPS PPP, which we expanded to accommodate the additional major diurnal/semidiurnal constituents considered here, as well as the use of both GPS and GLONASS data.

To do this, we used the CAMO site, the successor of CAMB used by Penna et al. (2015) and tested a range of coordinate and Zenith Wet Delay (ZWD) process noise settings exactly as described by Penna et al. (2015). We perform separate tests for GPS only, GLONASS only and GPS+GLONASS solutions. These tests focus on a range of metrics, namely the standard deviation of the height time series (shown as "Ht std/3", as divided by 3), the standard deviation of kinematic ZWD normalized by ZWD values from a static solution ("ZWDstatic"), root mean square of the carrier phase residuals ("RMSres"), ~~magnitude of~~ M_2 residual OTL magnitude, $\|Z_{res}\|$, ~~computed by differencing observed OTL with FES2004_GBe theoretical values ("M_2")~~ and $\|Z_{res}\|$ of a synthetic ~~~~~13.96 h signal and its controlled, known input (designated "synth err"). ~~The "synth err" $\|Z_{res}\|$ was estimated from solutions with harmonic signal introduced into sites' nominal location (2, 4 and 6 mm into east, north and up components respectively). The extracted amplitudes were then compared with the known signal to measure the level of propagation into other components.~~ We focus on the results without the introduction of this synthetic signal here.

For each of the major constituents, both diurnal and semi-diurnal, and for each of the constellation choices, we found that 3.2 mm/sqrt(s) for coordinate process noise and 0.1 mm/sqrt(s) for tropospheric zenith delay process noise were optimal for our solutions, the same values as identified by Penna et al. (2015) for M_2 using GPS only. Figure 2 shows the results of the tests, with the left panel showing the result of varying coordinate process noise while ZWD process noise was held fixed (0.1 mm/sqrt(s), a default value) and the right panel the result of varying the ZWD process noise with coordinate process noise equal to the optimum value of 3.2 mm/sqrt(s). The ~~only difference in our results to those of Penna et al. (2015) were for~~ finding of identical optimal process noise settings for all constituents and constellations suggests that the different amplitudes and frequencies are less important than the data noise in the ~~"synth err" test, where our results are inverted (but without changing the magnitude); the reason for this is discussed in detail in the supplementary material~~semidiurnal and diurnal frequency bands and that the constellation-specific data noise does not substantially vary between constellations.

5 Results and Discussion

5.1 ~~Effect of using GLONASS~~

Given the known accuracy of the ocean tide models in this region (Penna et al., 2015), and small effects of errors in solid Earth models, our assumption is that as $\|Z_{res}\|$ approaches zero as the estimates increase in accuracy, ~~as in Bos et al. (2015) .~~ also shown by Bos et al. (2015). Based on previous studies (e.g., Yuan et al., 2013) we expected $\|Z_{res}\|$ median values (up component) of ~2 mm for K_2 and K_1, ~1 mm for M_2, S_2, P_1 and ~0.5 mm for N_2, O_1, Q_1.

Figure 3 (upper panel) shows GPS, GLONASS and GPS+GLONASS $\|Z_{res}\|$ estimates for each of the east, north and up coordinate components. Over all components, the $\|Z_{res}\|$ are uniformly small for N_2, O_1 and Q_1, with median around 0.1 mm. Residuals are slightly higher for M_2, P_1 and S_2, median being around 0.5-0.7 mm, and are often noticeably higher for K_1 and K_2 although there is substantial variation by constellation.

The combined GPS+GLONASS solutions perform either at the same level as GPS AR (M_2, O_1, Q_1) or better (N_2, P_1) for the up component. $\|Z_{res}\|$ values are smaller and more consistent for the east (M_2, N_2, O_1) and north (M_2, N_2, P_1) components respectively. ~~Also, the~~ The GPS+GLONASS solution does not have $\|Z_{res}\|$ biases in the east and north components as is

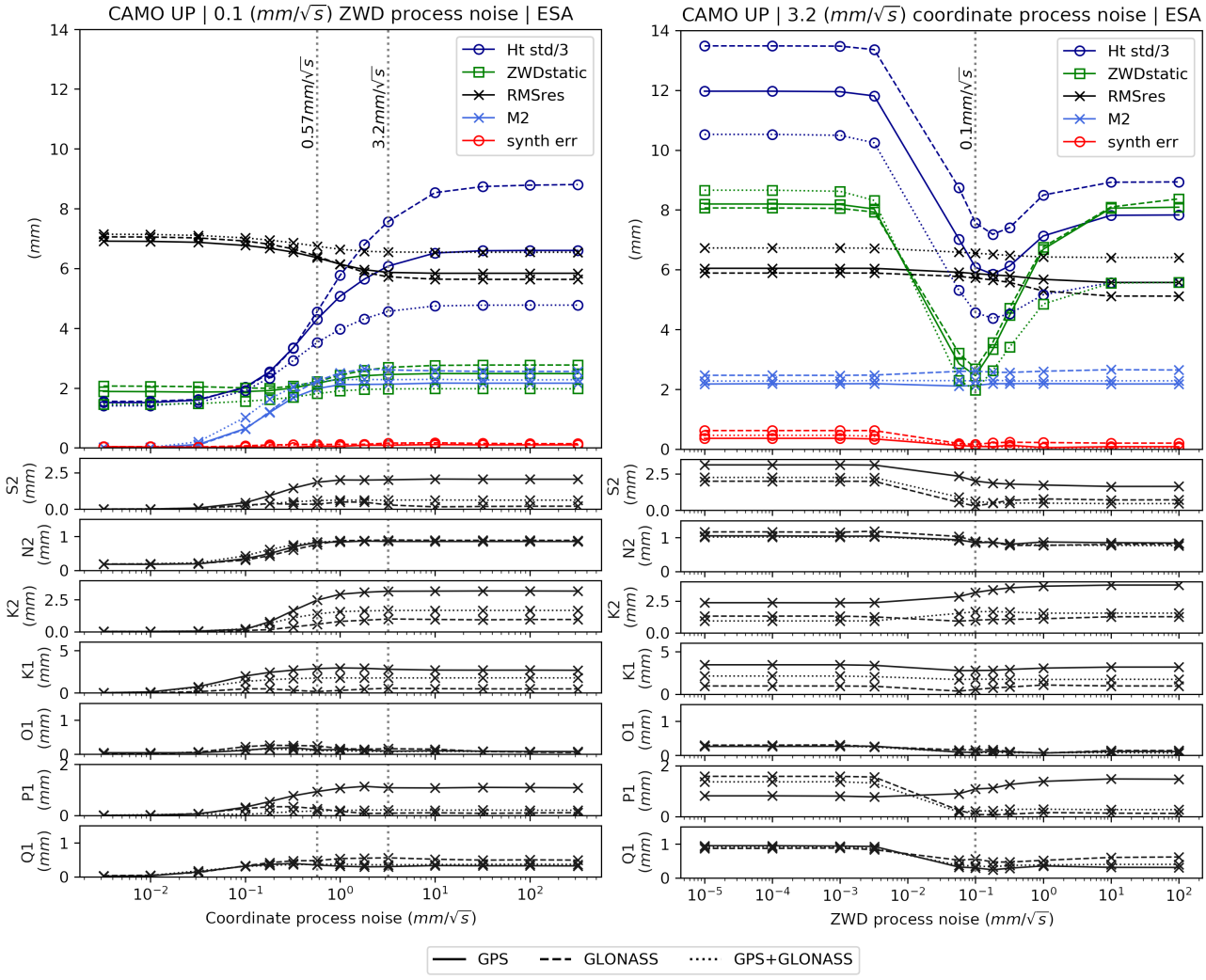

Figure 2. The effect of varying coordinate process noise (left) and ZWD process noise (right) at test site CAMO for the up component (2010.0 – 2014.0), performed with ESA repro2 products. ~~We expanded the tests of Penna et al. (2015) to include~~ $\|Z_{res}\|$ ~~of seven additional major constituents (S_2, N_2, K_2, K_1, O_1, P_1 and Q_1), named accordingly, and different constellations~~is relative to FES2004_GBe. The different constellations' configurations: GPS, GLONASS and GPS+GLONASS are presented as solid, dashed and dotted lines respectively. The colours pertain to the different metrics as described in the text and legend (note the same scheme is used as per Penna et al. (2015).

noticeable for the GPS AR solution (particularly for O_1 in east, and P_1 in north, respectively). By $\|Z_{res}\|$ bias we mean a noticeable gap between zero and the ~~distribution's lower bound (25th percentile - 1.5*interquartile range), which is present at all sites no matter how far inland~~lower whisker.

Considering the problematic GPS K_2 and K_1 constituents, the GPS AR can reasonably reliably, in comparison to other types of solutions, extract $\|Z_{res}\|$ in the east component (Figure 3, lower left panel) which is smaller than that of GLONASS

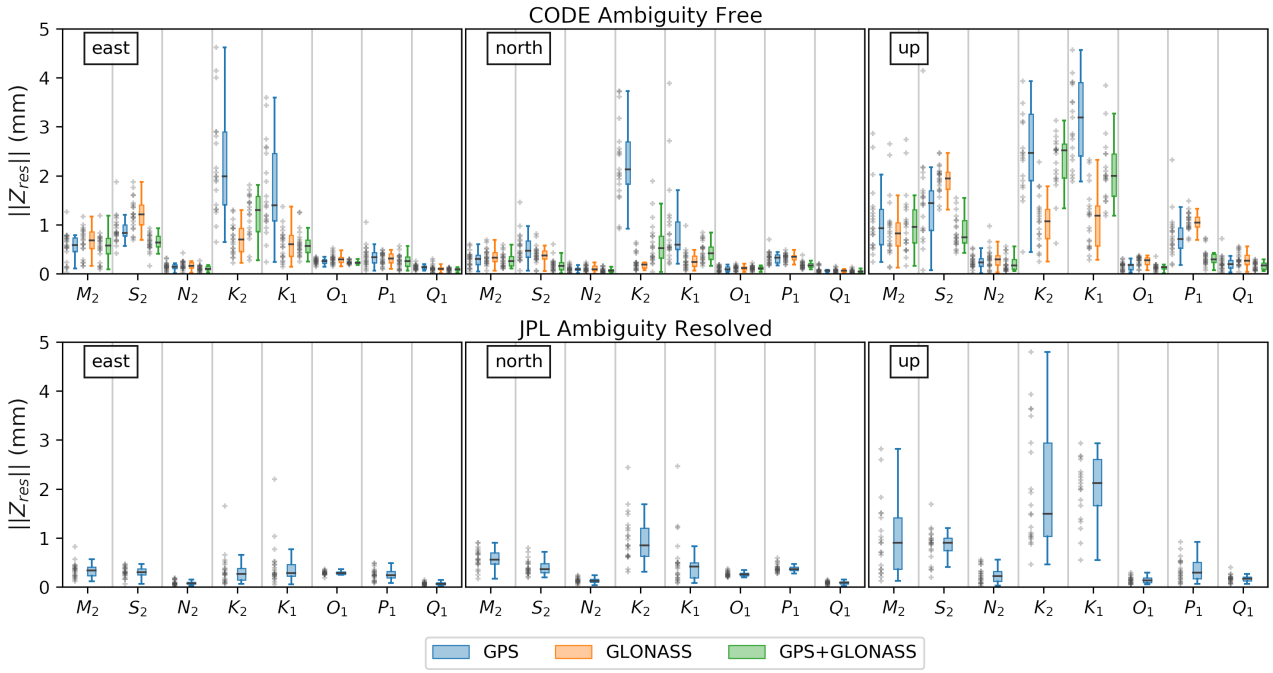

Figure 3. $\|Z_{res}\|$ per tidal constituent for east, north and up components (left, middle and right, respectively) relative to FES2014b_STW105d OTL values with CMC correction for JPL solutions. Grey crosses to the left of each boxplot represent sites' $\|Z_{res}\|$ values and are offset horizontally for clarity while the horizontal line over each boxplot is a median of each constituent's $\|Z_{res}\|$. Top: $\|Z_{res}\|$ for GPS, GLONASS and GPS+GLONASS PPP solutions (blue, orange and green, respectively) computed using CODE products. Bottom : $\|Z_{res}\|$ of the GPS AR solution computed with JPL native products. The boxes show the inter-quartile range and the whiskers mark the limit of an additional $\pm 1.5 \times$IQR, with median as a horizontal line

and GPS+GLONASS using ESA or CODE products. However, smallest $\|Z_{res}\|$ ~~extraction~~ in the up and north components is possible only using the GLONASS constellation solely which aligns with the conclusions of Abbaszadeh et al. (2020) who used ESA products and globally distributed GNSS network of sites.

Our results suggest that no single solution provides consistently better constituent estimates across all coordinate components. We suggest that optimum results are obtained using GPS+GLONASS for M_2, S_2, N_2, O_1, P_1 and Q_1, and GLONASS for K_2 and K_1, noting that GPS AR performs better for ~~the K_2 and K_1~~ all constituents in the east component.

We now explore the sensitivity of our solutions to different products and analysis choices ~~.~~ starting with elevation cutoff angle sensitivity, which particularly affects the amount of multipath influence on the coordinate time series. We pay particular attention to S_2, K_2, P_1 and K_1 given the large systematic errors evident in GPS only solutions. We follow with an inter-comparison of solutions using various products and then assess the impact of integer ambiguity resolution (GPS only). Finally, we test the stability of the constituent estimates to time series length.

5.1 Satellite orbit and clock products sensitivity tests

We assessed whether the solutions were sensitive to changes in satellite-elevation cutoff angle. Three additional cutoff angle scenarios were tested: 10°, 15° and 20° (in addition to the default 7° cutoff angle). Different elevation angle cutoffs will significantly alter the observation geometry as well as modulate the expression of signal multipath into solutions, decreasing the likely influence of multipath with higher cutoff values.

Figure 4 (top) shows the magnitude of vector ~~distance~~difference, $\|\Delta Z_{res}\|$, between ~~estimated~~ Z_{res} values estimated from the 7° and 20° solutions and CODE products in both cases (upper subplot). S_2, K_2, K_1 and P_1 constituents in the up coordinate component show ~~large mean vector distances~~ larger mean magnitudes of vector differences in both GPS (0.56, 2.29, 2.88, 0.54 mm, respectively) and GLONASS (0.82, 0.64, 1.01, 0.58 mm, respectively) with the rest of constituents showing differences of less than 0.5 mm. GPS+GLONASS ~~solution, up component, minimizes the~~ shows the smallest $\|\Delta Z_{res}\|$ ~~of~~ between 7° and 20° cutoff estimates for S_2 and P_1 (0.31, 0.23 mm, respectively) and ~~shows~~ an additional decrease in $\|\Delta Z_{res}\|$ for M_2, S_2,N_2, O_1, Q_1 in the up component. ~~For the horizontal coordinate components,~~ The high agreement between OTL values indicates the high stability of GPS+GLONASS ~~minimizes $\|\Delta Z_{res}\|$ for all constituents it increases the stability of all eight major constituents (including K_1 and K_2).~~ estimates with changing cutoff angles.

The same comparison ~~was done~~ for GPS AR (7° and 20° ~~solutions~~ (cutoff, JPL native products) ~~and~~ shows largely improved stability in comparison to ~~CODE's GPS solution which has effectively the same performance as with JPL's GPS only products~~ all GPS only ambiguity free solutions (Figure 4, bottom). However, K_2 up and K_1 up show substantial differences between solutions: K_2 ~~due to a lot tighter distribution~~ shows as much smaller variance of $\|Z_{res}\|$ distribution in the 20° solution, possibly due to removal of multipath, and K_1 ~~due to increased dispersion~~ shows an increased variance and median of $\|Z_{res}\|$ at increased cutoff angle.

Following Yuan et al. (2013), we assessed the possible influence of inconsistencies in precomputed orbits/clocks on estimated OTL displacements. This was done by computing $\|\Delta Z_{res}\|$ between pairs of solutions with common constellation configurations: GPS (no AR here) solutions computed using ESA, CODE and JPL products; GLONASS/GPS+GLONASS solutions using ESA and CODE products. ~~The importance of this assessment is directly related to the main principle of PPP technique: a priori knowledge of satellite-related parameters that are held fixed when estimating station coordinate time series. Given this approach, all satellite-related systematic errors will have at least partial expression into station-specific parameters (Yuan et al., 2013).~~

Figure 5 (top) shows the distribution of $\|\Delta Z_{res}\|$ between solutions computed with ESA and CODE products for all three constellation modes: GPS, GLONASS and GPS+GLONASS. The main differences are related to the S_2, K_2, K_1 and P_1 constituents. The maximum $\|\Delta Z_{res}\|$ between the observed OTL for the rest of the constituents is less than ~0.3 mm.

Compared with GPS JPL, both CODE and ESA solutions (Figure 5, middle and bottom, respectively) show $\|\Delta Z_{res}\|$ up to 0.5 mm in the horizontal components with respect to JPL solutions, which is also true for ESA in the up component with exception for K_2 and K_1. CODE shows similar behaviour to ESA, however, significant divergence from JPL (Figure 5, middle) is also observed for S_2 with even higher $\|\Delta Z_{res}\|$ for K_2 and K_1 in the up and the east.

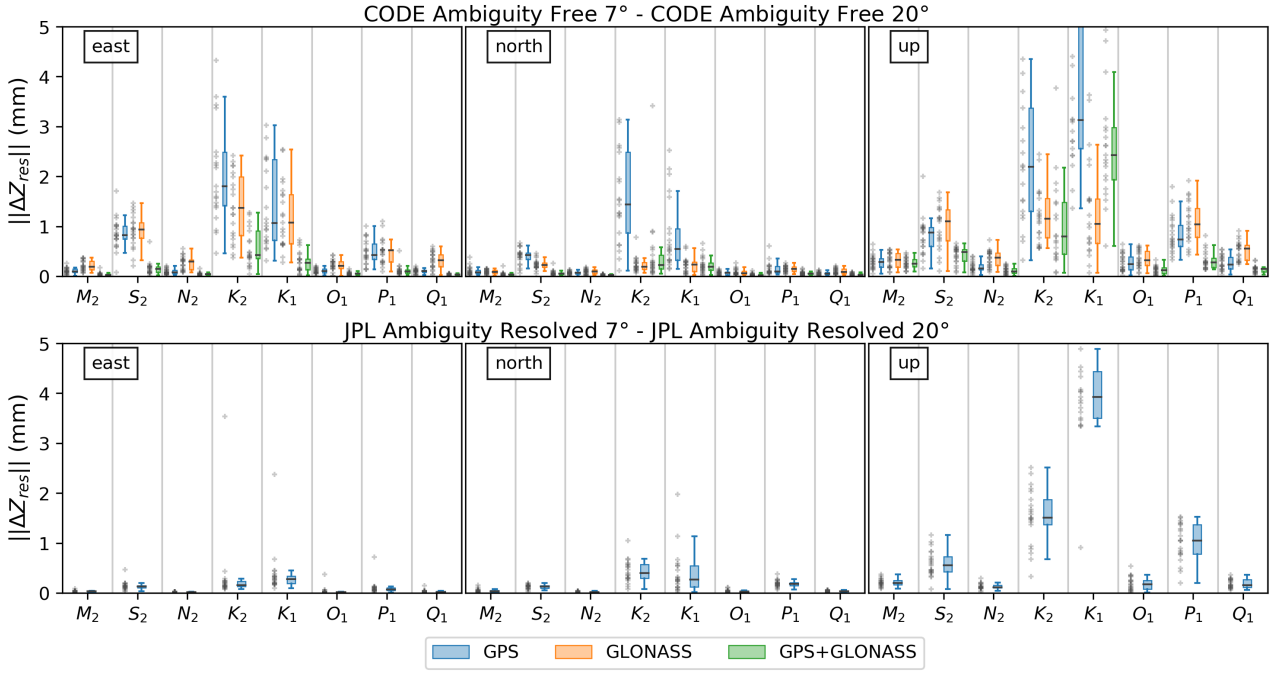

Figure 4. Magnitude of vector ~~distance~~ difference between estimated Z_{res} values computed with 7° and 20° elevation cutoff angles, $\|\Delta Z_{res}\|$, within the same set of orbits and clocks (top: CODE; bottom: JPL AR) for east, north and up coordinate components (left, middle and right, respectively). Grey crosses are as per figure 3. ~~Smaller~~ The smaller residuals ~~of~~ using CODE ~~'s~~ products with GPS+GLONASS (top) is a result of ~~better~~ improved OTL stability as a function of ~~OTL estimated with~~ cutoff angle using combined constellations ~~towards various cutoff angles~~ (except K_1 up and K_2 up). JPL's GPS AR also shows great stability with exception of K_2 up and K_1 up. $\|\Delta Z_{res}\|$ for GPS, GLONASS and GPS+GLONASS PPP solutions in blue, orange and green, respectively.

5.2 S_2 constituent

Focusing on S_2, the GPS up residual shows ~~~~1 mm residual bias between solutions using CODE and ESA products (compare blue records between left and right panels, Figure 6). The GPS $\|Z_{res}\|$ bias ~~is maintained~~ remains for solutions with a range of elevation cutoff angles (7°, 10°, 15° and 20°). GLONASS solutions (orange), however, show no $\|Z_{res}\|$ bias for ESA and ~~2~~ ~1.5 mm bias for CODE, both with 7° elevation angle. GLONASS bias values ~~in both cases~~ with both products increase with elevation cutoff angle up to 15°. This GLONASS dependency with elevation cutoff is present to a lesser degree in both east and north components and is the same with ESA and CODE products ~~.~~ (Fig. S5).

GPS $\|Z_{res}\|$ estimates show ~~inverse~~ similar behaviour in terms of $\|Z_{res}\|$ bias between ESA and CODE solutions in the up component (blue, Figure 6) ~~and an additional linear dependency of increasing~~ but ESA solutions' median $\|Z_{res}\|$ ~~as a function of increasing elevation cutoff in the north component~~values are ~1 mm larger for all elevation cutoff angle solutions. Both ESA and CODE GPS+GLONASS S_2 results (green, Figure 6) show a blend of the two patterns observed with GPS and

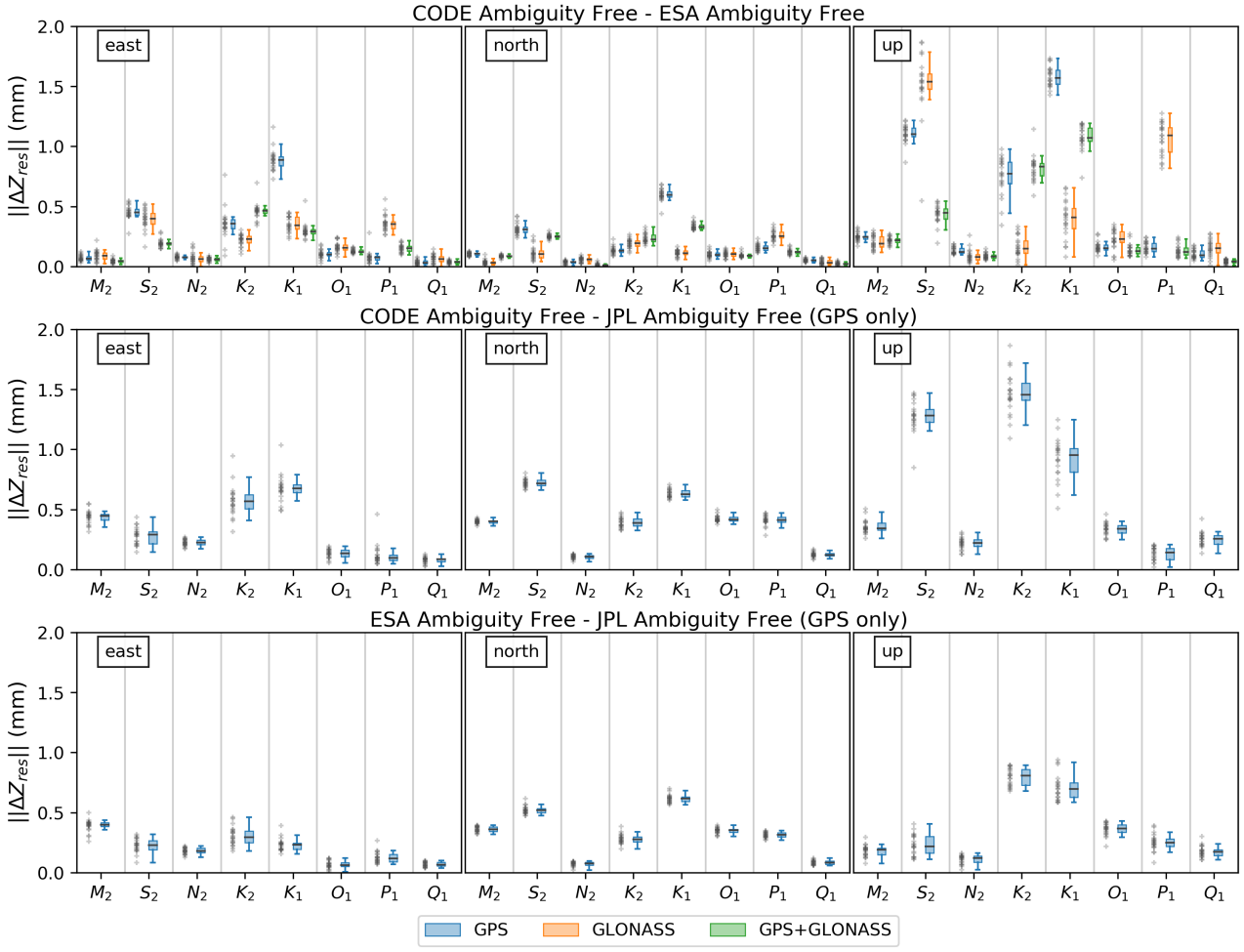

Figure 5. OTL vector differences between CODE, ESA and JPL solutions (ambiguity free). Top: GPS, GLONASS and combined GPS+GLONASS differences between CODE and ESA solutions; Middle: GPS difference between CODE and JPL solutions (ambiguity free); Bottom: GPS difference between ESA and JPL solutions (ambiguity free). Note the vertical scale of 2 mm. Grey crosses are as per Figure 3.

GLONASS solutions. GPS+GLONASS S_2 shows less sensitivity to the cutoff angle change than ~~the GLONASS solutions with both products. However, the CODE GPS+~~GLONASS ~~S_2 solution consistently produces smaller $\|Z_{res}\|$ biases which may be related to the absence of $\|Z_{res}\|$ bias in the GPS solution and its higher weight in the solution due to higher number of simultaneously visible SVs. The effect was also studied with JPL products and AR: GPS and GPS AR; see Sect. 5.7.~~ or GPS solutions alone.

The substantial difference in S_2 between ESA and CODE (Figure 6) suggests important differences in raw GNSS data analysis approaches within respective Analysis Centres. One ~~possible explanation is associated with the treatment of S1~~ relevant

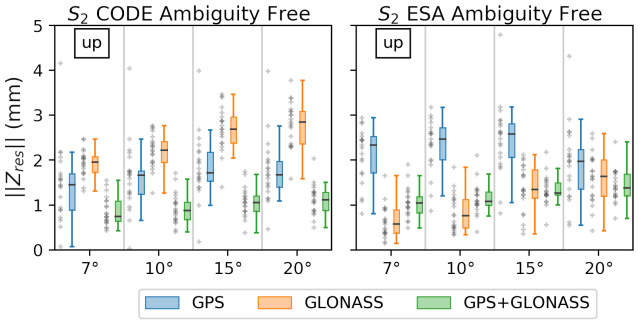

Figure 6. GPS, GLONASS and GPS+GLONASS $\|Z_{res}\|$ for the S_2 constituent in the up component as a function of elevation cutoff angle, computed with ESA (left) and CODE products (right). Note the inverse behaviour of GPS and GLONASS biases and the linear dependence of the GLONASS biases. Grey crosses are as per Fig. 3.

difference between products is in treatment of S_1 and S_2 atmospheric tides which were corrected for at the observation level in CODE products ~~(no correction in ESA)~~but not in ESA. However, the ~~total value of the vector difference cannot be explained by unmodelled atmospheric tides alone. Additionally, the~~ inverse behaviour of GPS and GLONASS between ESA and CODE solutions (orange, Figure 6) cannot be explained with a single correction applied to both constellations. We expect that the differences in each solution are a function of satellite orbit modelling, although the ~~issue~~ exact origin is not clear and needs further investigation.

5.3 K_2 and K_1 constituents

~~Like 7° CODE and ESA solutions, $\|\Delta Z_{res}\|$~~ As seen from Fig. 3, $\|Z_{res}\|$ can be minimized if using GLONASS for the extraction of K_1 and K_2 constituents and GPS+GLONASS for the remainder of the constituents. In this case, ~~$\|\Delta Z_{res}\|$~~ $\|Z_{res}\|$ will stay below 0.25 mm for north components and below 0.5 mm for the east and the up components.

GLONASS K_2 and K_1 estimates in the north have the ~~tightest distribution of the~~ lowest variance in $\|Z_{res}\|$ ~~,~~and are most stable ~~for the range of~~ with different elevation cutoff angles and products. For the east component, CODE products ~~GLONASS struggles to compete~~ with GLONASS have larger $\|Z_{res}\|$ median and scatter than with GPS+GLONASS for K_1 and in terms of ~~minimised distribution of $\|Z_{res}\|$ (K_1) and~~ elevation cutoff stability (K_2 and K_1). ~~The GLONASS~~ Solutions using the ESA GLONASS products, however, perform better for K_1 east ~~is not true for the ESA products solutions which overperform the~~ than the respective GPS+GLONASS in terms of $\|Z_{res}\|$ distribution consistency and median (~~see supplementary Figure S_2)and this explains the minor difference between ESA and CODE GLONASS solutions (Figure 5, top left)~~Fig. S2). Elevation cutoff stability of ESA K_2 and K_1 in the east component is ~~exactly as with CODE –~~ best with GPS+GLONASS as also found when using CODE products.

The up component of K_2 and K_1 is the most problematic, showing high $\|Z_{res}\|$ values with all constellation modes. GLONASS OTL values ~~from both ESA and CODE solutions have tightest distributions and smallest~~ using either both ESA or CODE products have the smallest medians and variances of $\|Z_{res}\|$~~median values overperforming~~ , outperforming JPL GPS

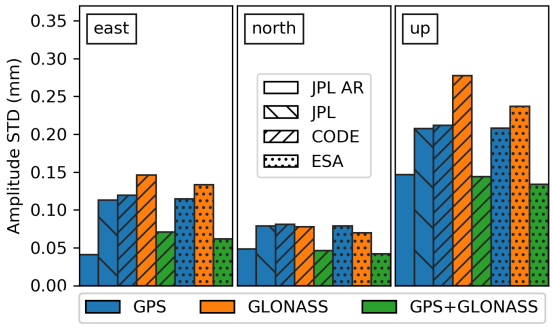

Figure 7. Average uncertainties (1-sigma) for OTL amplitudes computed across eight OTL constituents per products (stipple) and processing modes/constellation (colour): GLONASS (orange) and GPS (blue) modes show higher 1-sigma uncertainties~~STDs~~, while GPS-only AR and combined GPS+GLONASS (green) show minimum 1-sigma uncertainties with exception for east.

AR. Note that GPS+GLONASS K_2 up has a marginally smaller median $\|\Delta Z_{res}\|$ in the elevation cutoff test than that of GLONASS only, possibly due to ~~higher amount of SVs~~the larger number of total satellites, however, both K_2 and K_1 $\|Z_{res}\|$ ~~values recovered are too high with major differences between CODE and ESA products' values~~suggest a ~1.5 mm bias.

While we cannot ~~certainly~~ definitively select a single constellation configuration optimal for all components of K_2 and K_1, we can conclude that based on our analysis, GLONASS ~~performs best~~ solutions have smaller $\|Z_{res}\|$ in the K_2 and K_1 north and up components while ~~east component might show~~ the east component shows better results with GPS+GLONASS (K_1, CODE)~~but, due to better consistency between products, GLONASS values are still preferred~~. However, we recommend GLONASS-only solutions due to the higher level of agreement between solutions using ESA and CODE products. The only exception ~~to~~ is the east component ~~conclusions is~~ where the preference is for JPL GPS AR (see Sect. 5.7).

5.4 P_1 constituent

~~The high $\|\Delta Z_{res}\|$ in~~ GLONASS P_1 ~~constituent~~ constituents show high $\|\Delta Z_{res}\|$ between CODE and ESA solutions over all coordinate components (orange, Figure 5 top)~~is~~. This was unexpected as ESA and CODE $\|Z_{res}\|$ boxplots show similar distributions of values (see Figure ~~S_2 in~~ S2 in the supplementary material for the equivalent ESA boxplots). This suggests a symmetrical deviation from the modelled values that produces a high $\|\Delta Z_{res}\|$. In all cases, however, GPS+GLONASS is preferred for P_1 estimation.

5.5 Effect of different orbit and clock products on noise and uncertainty

Changing orbit and clock products also changes the time series noise characteristics and hence influences the uncertainties of the estimated constituents (estimated separately by Eterna for amplitude, Figure 7 and phase, Figure 8). Amplitude uncertainties are expressed here as an average across all constituents as they do not differ much between analysed constituents. ETERNA assumes a white noise model in its analysis. We conclude that GLONASS solutions produce the highest amplitude uncertainties

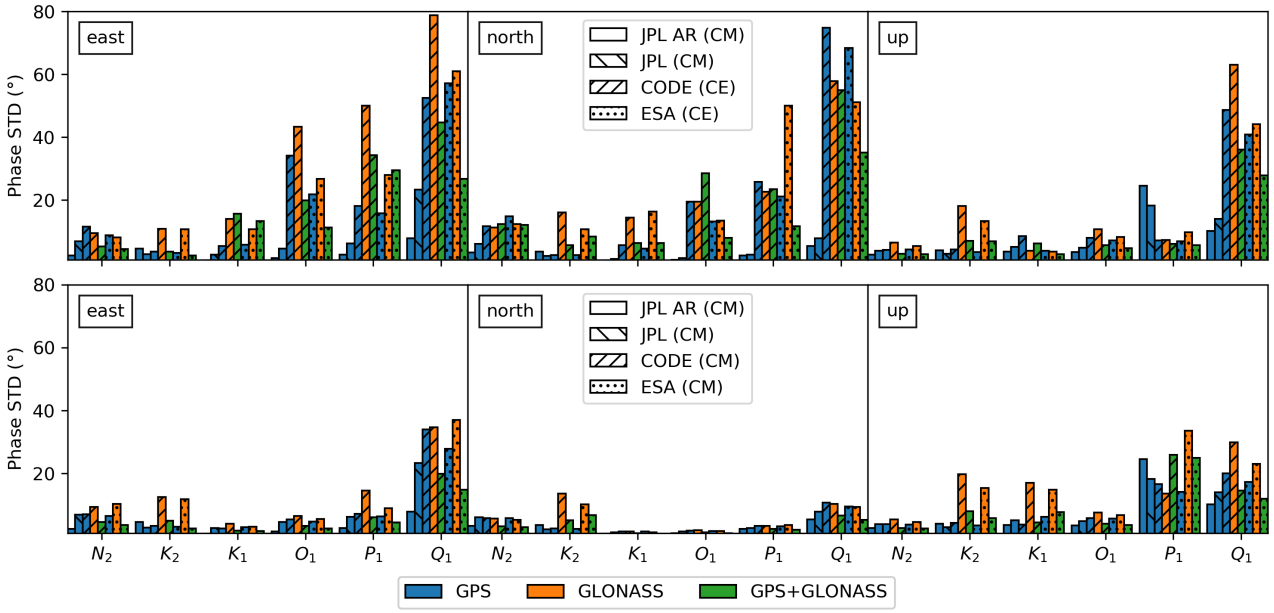

Figure 8. Average phase ~~STD (~~uncertainty ~~)~~ per constituent for different products as returned by Eterna. ESA and CODE products were in CE frame by default (top) and converted to CM (bottom) while JPL are in CM in both. M_2 and S_2 phase ~~STDs~~ 1-sigma uncertainties are not shown here as values are too small to be seen with the scale specified.

for east (0.15 mm CODE, 0.14 mm ESA) and up components (0.22 mm CODE, 0.27mm ESA) while showing the same uncertainty as GPS for the north (0.07 mm, both CODE and ESA). GLONASS ~~amplitude uncertainties from~~ solutions using CODE products tend to ~~be~~ have amplitude uncertainties that are marginally higher than those of ESA products. The amplitude uncertainties for combined GPS+GLONASS solutions are equal to those of JPL with ambiguities fixed (GPS AR), although the JPL GPS AR solution has slightly smaller uncertainty in the east component (smaller by ~~~~0.02 mm).

Considering the uncertainties of phase values, these are unsurprisingly dependent on the constituent's amplitude. Because JPL native products ~~show a significant advantage in this case when compared to~~ are in a CM frame, the constituent amplitudes are larger at the time of ETERNA analysis than those using ESA and CODE ~~due to differences in frames: CM (JPL) and CE (~~products which are both provided in a CE frame. For the ESA and CODE ~~). This~~ solution, this results in up to an order of magnitude increase in phase uncertainties for "weaker" diurnal constituents in the region: N_2, O_1, P_1, Q_1 (Figure 8).

In general, this frame effect is directly related to centre of mass correction (CMC) specific to the constituent's CMC vector in comparison to the total theoretical OTL vector. If applying a CMC correction to the constituent increases its amplitude, phase STD values will decrease in ~~CM-frame~~ a CM frame solution. This is critically important for the constituents with amplitudes below 0.5 mm, as phase uncertainty increases significantly below this threshold. The most significant exception in our dataset is P_1 in the up component which has a much larger amplitude in CE frame (Figure 8, right in top and bottom).

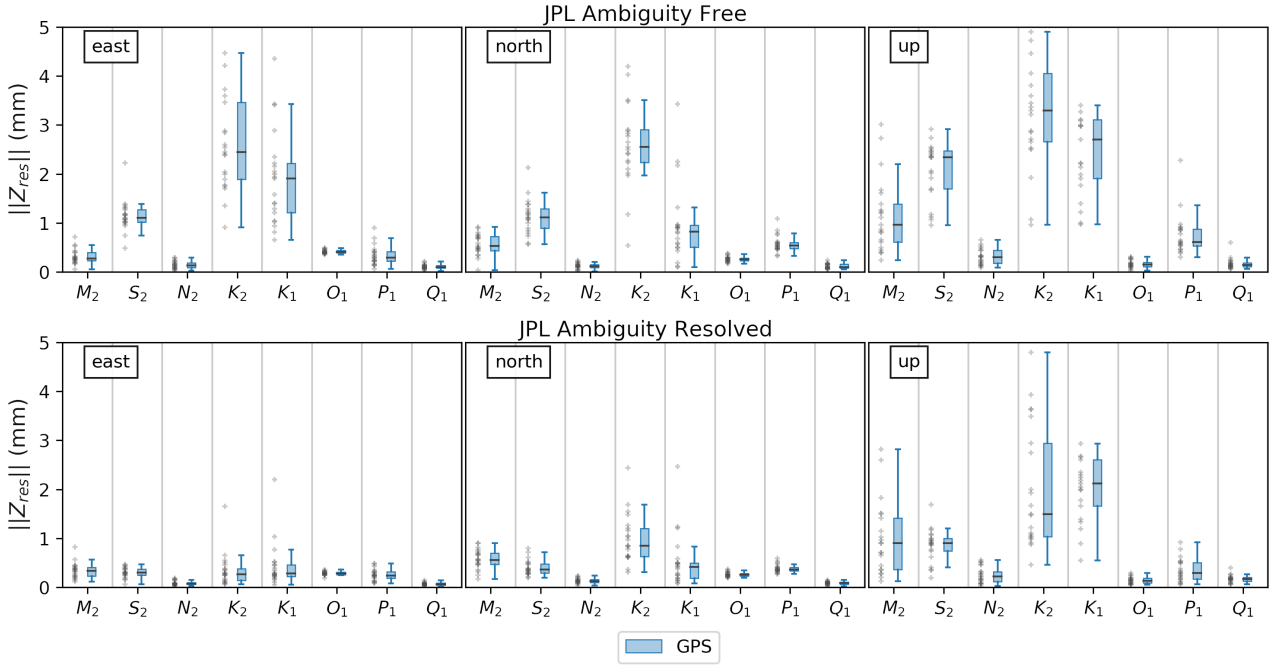

Figure 9. Comparison of residual constituents' estimates from GPS (top) and GPS AR (bottom) JPL native solutions. Grey crosses are as per Figure 3. As seen, most of constituents' $\|Z_{res}\|$ ~~distributions became tighter~~ distribution variances and medians are smaller while S_2 $\|Z_{res}\|$ bias ~~got~~ is removed with ~~enabling of~~ AR solutions.

Converting CE products to CM (Figure 8, bottom) was done to demonstrate that the changes in phase uncertainty are indeed introduced by the smaller amplitudes in the CE frame. While this holds true, it is obvious that ~~not only does the P1~~ the P_1 up phase uncertainty ~~increase~~increases, as was expected based on comparison with the JPL solutions. GLONASS K_1 up phase uncertainties show almost an order of magnitude increase in the CM frame while having unexpectedly small values in CE. This is a direct cause of GLONASS solution having larger K_1 up amplitudes in CE and smaller in CM with both CODE and ESA.

5.6 Impact of Ambiguity Resolution on GPS

The multi-GNSS products used here do not allow integer AR with PPP and this is an active area of research and development within the IGS. However, assessing the impact of AR on GPS-only solutions provides some insight towards the future benefit of AR on GLONASS and GPS+GLONASS solutions once such products become available. We compared OTL residuals from GPS and GPS AR using JPL native products that contain wide lane and phase bias tables (WLPB files) required for integer AR with PPP.

Figure 9 shows the effect on estimated constituents from enabling AR in a standard solution with 7° cutoff. Here we observe decreased $\|Z_{res}\|$ over all coordinate components compared with the estimates from a non-AR solution. This is most visible in the K_2 and K_1 constituents and in the elimination of the S_2 $\|Z_{res}\|$ bias and with smaller improvements in M_2 and P_1.

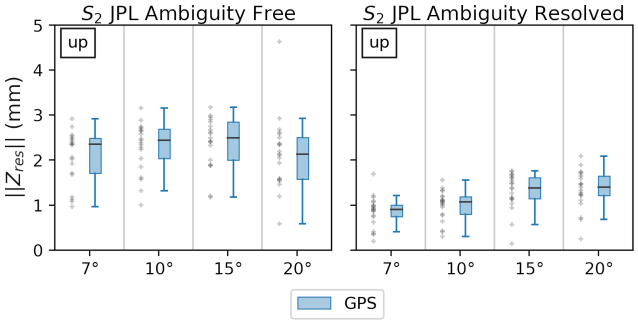

Figure 10. GPS S_2 up constituent's $||Z_{res}||$ change with elevation cutoff angle computed with JPL products floating AR (left) and integer AR (right). Grey crosses are as per Figure 3. As seen, AR ~~completely removes~~ helps in removing the bias and ~~slightly improves overall consistency between stations~~decreases the $||Z_{res}||$ distribution variance.

Importantly, Figure 9 shows that enabling AR eliminates $||Z_{res}||$ bias in GPS and aligns the residual vectors with ESA/CODE GPS+GLONASS (Figure 3). ~~Thus~~This is a clearer improvement than reported by Thomas et al. (2006).

Given this effect, the S_2 $||Z_{res}||$ bias was once again assessed with various elevation cutoff angles solutions. JPL GPS solutions (floating AR), in the up component (Figure 10, left), show the S_2 $||Z_{res}||$ bias to be constant ~~between cutoff angles at~~ with cutoff angle, being about 1 mm~~with median~~ , and with the $||Z_{res}||$ ~~fluctuating~~ variance of around 3 mm. Similar behaviour was previously observed with solutions using ESA products (Fig.6).

Enabling integer ambiguity resolution (GPS AR) removes the ~1 mm S_2 $||Z_{res}||$ bias completely ~~over all tested~~ at 7° and 10° elevation cutoff angles while ~~introducing a slight increase of the median residual magnitude~~ leaving ~ 0.4 mm bias at 15° and 20° in the up component~~with increasing elevation cutoff~~ . Consequently, up $||Z_{res}||$ medians change by 1-2 mm depending on elevation cutoff angle. Based on this observation, we expect that ~~utilising ambiguity resolution~~ resolving ambiguities within PPP might help in solving, or at least minimising, the S_2 $||Z_{res}||$ present in ESA GPS and CODE GLONASS solutions. Eliminating biases in GPS and GLONASS separately should increase the stability and consistency of GPS+GLONASS S_2 $||Z_{res}||$.

5.7 Impact of timeseries length

~~Yuan et al. (2013) used~~ Yuan et al. (2013) used a filter based harmonic parameter estimation approach and ~~demonstrated~~ examined the dependence of Kalman filter convergence ~~and~~ on timeseries length for each of the eight major constituents. ~~Yuan et al. (2013) concluded that~~Yuan et al. (2013) concluded that, after 1000 daily solutions, convergence (minimized $||Z_{res}||$) was reached for lunar-only constituents (M_2, N_2, O_1, Q_1) while reporting solar-related constituents (S_2, K_2, K_1, P_1) were not fully converged even after 3000 daily solutions.

~~Here, we~~ We assessed how $||Z_{res}||$ of each of 8 major constituents vary as a function of the time series length with kinematic estimation approach. The duration of the series varied by ~~integral years , and~~integer years and, to enable a complete analysis, we expanded the candidate solutions to 2019.0 and processed additional data with operational products: JPL repro3.0, ESA

operational, CODE MGEX (CODE operational lack GLONASS clock corrections). ~~Importantly, the results shown in Figure 11 are therefore a composition of reprocessed products and operational products (years 5 to 9); the design of the reprocessed solutions should closely match the operational products .~~

~~Dependency of estimated $\|Z_{res}\|$ and timeseries' length in years for two solar related constituents: S_2 (top), K_1 (bottom). GPS, GLONASS and GPS+GLONASS PPP solutions in blue, orange and green, respectively using ESA products. Grey crosses are as per Figure 3. Note that 1 to 4 years of timespan use ESA repro2 while the rest uses a combination of ESA repro2 and ESA operational products. Figure 11 shows that even three-years of data appears to be sufficient to get reliable $\|Z_{res}\|$ values for GLONASS for K_1 and GLONASS or GPS+GLONASS for S_2 (see Supplementary Figure S3).~~

~~Changing~ While the goal of a reprocessing campaign is to preserve consistency with operational products (Griffiths, 2019), based on previous results, we assumed that changing satellite orbit and clock products may produce substantial differences in ~~results~~problematic solar-related constituents (S_2, K_2, K_1, P_1). Thus, we first performed a comparison of ESA repro2 solutions (2010.0-2014.0) with the ESA operational product (2014.0-2019.0) which ~~showed no significant changes in terms of $\|\Delta Z_{res}\|$ for M_2, N_2, O_1, P_1 and Q_1 estimated (Figure 12~~confirmed the hypothesis (Figure 11). GLONASS ~~, however, shows significant difference between two datasets~~ $\|\Delta Z_{res}\|$ show the smallest variance for K_1 and K_2 compared with GPS and GPS+GLONASS but are significant, up particularly, ~~up specifically,~~ which might be related to the changes in ~~GLONASS products processing. Considering the~~ the analysis used to produce GLONASS orbits and clocks. Considering S_2, ~~$\|\Delta Z_{res}\|$ shows~~ the very same form of bias remains as previously seen ~~with~~ in the 2010.0-2014.0 dataset~~which suggests~~. This suggests a symmetric deviation of repro2 and operational products solutions from the modelled value. The same explanation can be applied to the GPS-only P_1 $\|\Delta Z_{res}\|$ bias in the up component of 0.5 mm.

The results shown in Figure 12 are produced from a composition of reprocessed products and operational products (years 5 to 9). We focus on S_2 up and K_1 up, as the most problematic diurnal constituents. The results align with general conclusions of Yuan et al. (2013) suggesting a weak relationship between timeseries length and $\|Z_{res}\|$ for solar-related constituents. However, if constituents are examined according to our recommended optimum constellation strategy, $\|Z_{res}\|$ appears (see Fig. S4) stable over time, which suggests that even if there are changes in the products, they are not having an impact with this methodology.

6 Conclusions

We expand the GPS-only methodology of ocean tide loading displacement estimation described in Penna et al. (2015) with ~~GLONASS constellation and~~ data from the GLONASS constellation. We assess the performance of GPS and GLONASS for the estimation of eight major ocean tide loading constituents in stand-alone modes and in a combined GPS+GLONASS mode. We examine data from 21 sites from the UK and western Europe over a period of 2010.0-2014.0 through processing data in kinematic PPP using products from three different analysis centres: CODE, ESA and JPL. The latter was also used to assess the effect of GPS ambiguity fixing on estimated ocean tide loading ~~displacement~~displacements. All solutions were ~~intercompared~~

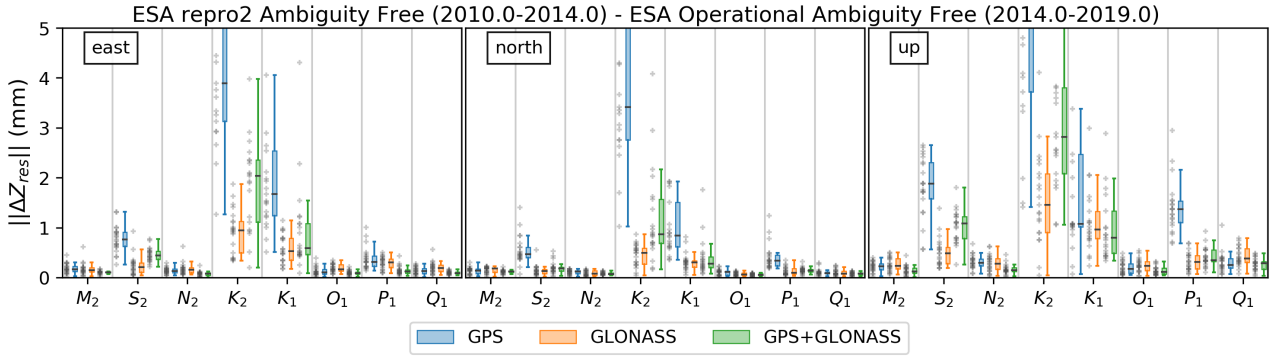

Figure 11. OTL vector differences between ESA repro2 (2010.0-2014.0) and ESA operational (2014.0-2019.0) OTL estimates: GPS (blue), GLONASS (orange), GPS+GLONASS (green) constellation modes present. Grey crosses are as per Figure 3.

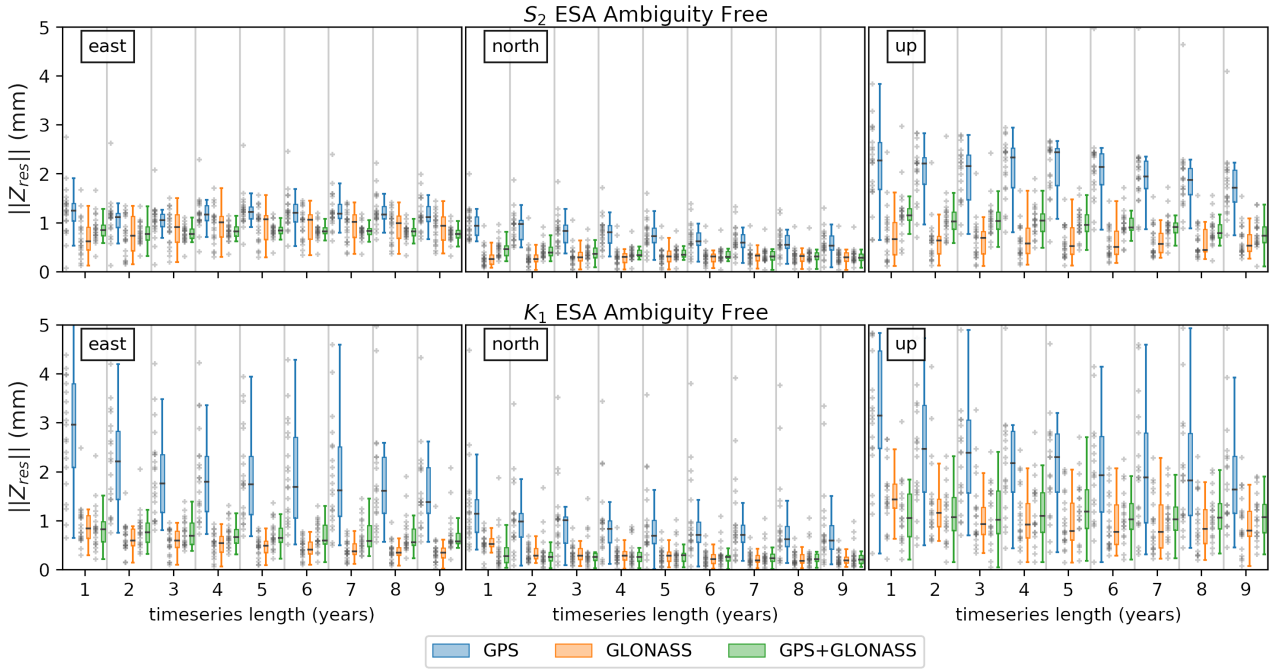

Figure 12. Dependency of estimated $\|Z_{res}\|$ and timeseries' length in years for two solar related constituents: S_2 (top), K_1 (bottom). GPS, GLONASS and GPS+GLONASS PPP solutions in blue, orange and green, respectively using ESA products. Grey crosses are as per Figure 3. Note that 1 to 4 years of timeseries length use ESA repro2 while the rest uses a combination of ESA repro2 and ESA operational products.

inter-compared to gain an insight into the sensitivities of the constituent estimates to different choices of satellite orbit and clock products, satellite elevation cutoff, and constellation configurations.

We find that ~~no single constellation mode solution for~~ the optimal constellation mode varies across all eight major tidal constituents ~~exists. However, we do find that GLONASS-based estimates show a comparable level of performance to ambiguity-free GPS for M_2, N_2, O_1, P_1 and Q_1 while showing improved results for K_2~~ and ~~K_1. Alternatively, this optimal solution can be constructed from the combination of constellation modes for each constituent and component for the case of GPS and GLONASS presence.~~

components. We show that ambiguity-free GPS+GLONASS solutions show a similar level of precision as GPS with ambiguities resolved (GPS AR), with P_1 estimates using GPS+GLONASS showing improved precision and stability. The K_2 and K_1 constituents, which are known to be problematic in GPS solutions, are still unusable in GPS+GLONASS solutions, ~~due to~~ presumably due to the propagation of GPS related errors. The S_2 constituent also cannot be reliably recovered with GPS+GLONASS as GLONASS shows dependency between ~~estimates and~~ the estimates and the chosen elevation cutoff angle. GPS-based estimates of S_2 show a constant bias in absolute residuals when ambiguity resolution is not implemented, but this is ~~removed~~ substantially reduced by resolving the ambiguities to integers. GLONASS-based estimates show a comparable level of performance to ambiguity-free GPS for M_2, N_2, O_1, P_1 and Q_1 while showing improved results for K_2 and K_1.

Additional comparison of OTL estimates from reprocessed and operational products shows that GLONASS estimates of K_2 and K_1 show differences in the up and, to the lesser extent in the east, components when using different products.

Considering the above, we suggest that estimation of K_1 and K_2 constituents is best undertaken using GLONASS only solutions with an emphasis towards the north component where it is most stable. M_2, S_2, N_2, O_1 and Q_1 can be reliably estimated from combined GPS+GLONASS or GPS AR solutions while P_1 is best with GPS+GLONASS.

Integer ambiguity resolution was not possible in the GLONASS or GPS+GLONASS solutions tested here due to limitations in the products available. However, evidence from our GPS AR testing suggests that further increases in precision and stability will be seen when AR fixing can be performed ~~which~~ using GLONASS, and this should have a positive impact on estimates of solar-related constituents.

Code and data availability. GNSS data were obtained from the Natural Environment Research Council (NERC) British Isles continuous GNSS Facility (BIGF), www.bigf.ac.uk and the International GNSS Service (IGS), www.igs.org. OTL values and TPXO7.2 OTL grid were obtained from free ocean tide loading provider, holt.oso.chalmers.se/loading/. CODE REPRO_2015 and CODE MGEX orbit and clock products were obtained from the University of Bern, ftp.aiub.unibe.ch/REPRO_2015/ and ftp.aiub.unibe.ch/CODE_MGEX/ respectively, ESA repro2 and operational from the Crustal Dynamics Data Information System (CDDIS), JPL repro 2.1 and repro 3.0 from NASA Jet Propulsion Laboratory, sideshow.jpl.nasa.gov/pub/.

GipsyX binaries were provided under license from JPL. Eterna tidal analysis and prediction software with source code was acquired from International Geodynamics and Earth Tide Service (IGETS), igets.u-strasbg.fr/soft_and_tool.php. The source code of GipsyX wrapper developed to facilitate the processing, analyse output and undertake plotting can be found at: github.com/bmatv/GipsyX_Wrapper.

Author contributions. BM facilitated processing of the GNSS data with GipsyX and analysis of the resulting timeseries under the supervision of MK and CW. All authors contributed to the discussion of the results and writing of the manuscript.

Competing interests. The authors declare that they have no conflicts of interest.

Acknowledgements. The services of the Natural Environment Research Council (NERC) British Isles continuous GNSS Facility (BIGF), www.bigf.ac.uk, in providing archived GNSS data to this study, are gratefully acknowledged. We are grateful to NASA Jet Propulsion Laboratory for the GipsyX software, products and support. We thank IGS, www.igs.org, for providing GNSS data and ESA reprocessed products; CODE, www.aiub.unibe.ch, for providing reprocessed products. We thank Klaus Schueller for advice and discussion on Eterna software. The services of TPAC High Performance Computing Facility are acknowledged gratefully. We gratefully acknowledge Machiel Bos whose support and discussion were vital for the project. We thank the Free Ocean Loading Provider for the OTL computation services and for providing the OTL grid that was used in Figure 1.

References

Abbaszadeh, M., Clarke, P. J., and Penna, N. T.: Benefits of combining GPS and GLONASS for measuring ocean tide loading displacement, Journal of Geodesy, 94, 63, https://doi.org/10.1007/s00190-020-01393-5, 2020.

Agnew, D. C.: Earth Tides, pp. 151–178, https://doi.org/10.1016/b978-0-444-53802-4.00058-0, 2015.

Allinson, C. R.: Stability of direct GPS estimates of ocean tide loading, Geophysical Research Letters, 31, https://doi.org/10.1029/2004gl020588, 2004.

Baker, T. F.: Tidal Deformations of the Earth, Science Progress, 69, 197–233, 1984.

Bar-Sever, Y. E., Kroger, P. M., and Borjesson, J. A.: Estimating horizontal gradients of tropospheric path delay with a single GPS receiver, Journal of Geophysical Research: Solid Earth, 103, 5019–5035, https://doi.org/10.1029/97jb03534, 1998.

Bertiger, W., Desai, S. D., Haines, B., Harvey, N., Moore, A. W., Owen, S., and Weiss, J. P.: Single receiver phase ambiguity resolution with GPS data, Journal of Geodesy, 84, 327–337, https://doi.org/10.1007/s00190-010-0371-9, 2010.

Blewitt, G.: Self-consistency in reference frames, geocenter definition, and surface loading of the solid Earth, Journal of Geophysical Research: Solid Earth, 108, https://doi.org/10.1029/2002jb002082, 2003.

Boehm, J., Werl, B., and Schuh, H.: Troposphere mapping functions for GPS and very long baseline interferometry from European Centre for Medium-Range Weather Forecasts operational analysis data, Journal of Geophysical Research: Solid Earth, 111, https://doi.org/10.1029/2005jb003629, 2006.

Bos, M. S.: Ocean Tide Loading Using Improved Ocean Tide Models, Thesis, University of Liverpool, 2000.

Bos, M. S. and Baker, T. F.: An estimate of the errors in gravity ocean tide loading computations, Journal of Geodesy, 79, 50–63, https://doi.org/10.1007/s00190-005-0442-5, 2005.

Bos, M. S., Penna, N. T., Baker, T. F., and Clarke, P. J.: Ocean tide loading displacements in western Europe: 2. GPS-observed anelastic dispersion in the asthenosphere, Journal of Geophysical Research-Solid Earth, 120, 6540–6557, https://doi.org/10.1002/2015jb011884, 2015.

Boy, J. P., Llubes, M., Hinderer, J., and Florsch, N.: A comparison of tidal ocean loading models using superconducting gravimeter data, Journal of Geophysical Research: Solid Earth, 108, https://doi.org/10.1029/2002jb002050, 2003.

Dziewonski, A. M. and Anderson, D. L.: Preliminary reference Earth model, Physics of the Earth and Planetary Interiors, 25, 297–356, https://doi.org/10.1016/0031-9201(81)90046-7, 1981.

Farrell, W. E.: Deformation of the Earth by surface loads, Reviews of Geophysics, 10, https://doi.org/10.1029/RG010i003p00761, 1972.

Foreman, M. G. G. and Henry, R. F.: The harmonic analysis of tidal model time series, Advances in Water Resources, 12, 109–120, https://doi.org/10.1016/0309-1708(89)90017-1, 1989.

Fu, Y., Freymueller, J. T., and van Dam, T.: The effect of using inconsistent ocean tidal loading models on GPS coordinate solutions, Journal of Geodesy, 86, 409–421, https://doi.org/10.1007/s00190-011-0528-1, 2012.

Griffiths, J.: Combined orbits and clocks from IGS second reprocessing, J Geod, 93, 177–195, https://doi.org/10.1007/s00190-018-1149-8, 2019.

Griffiths, J. and Ray, J. R.: On the precision and accuracy of IGS orbits, Journal of Geodesy, 83, 277–287, https://doi.org/10.1007/s00190-008-0237-6, 2009.

Ito, T. and Simons, M.: Probing asthenospheric density, temperature, and elastic moduli below the western United States, Science, 332, 947–51, https://doi.org/10.1126/science.1202584, 2011.

Jentzsch, G.: Earth tides and ocean tidal loading, pp. 145–171, Springer-Verlag, https://doi.org/10.1007/bfb0011461, 1997.

Johnston, G., Riddell, A., and Hausler, G.: The International GNSS Service, book section Chapter 33, pp. 967–982, https://doi.org/10.1007/978-3-319-42928-1_33, 2017.

Khan, S. A. and Tscherning, C. C.: Determination of semi-diurnal ocean tide loading constituents using GPS in Alaska, Geophysical Research Letters, 28, 2249–2252, https://doi.org/10.1029/2000gl011890, 2001.

King, M. A.: Kinematic and static GPS techniques for estimating tidal displacements with application to Antarctica, Journal of Geodynamics, 41, 77–86, https://doi.org/10.1016/j.jog.2005.08.019, 2006.

King, M. A. and Aoki, S.: Tidal observations on floating ice using a single GPS receiver, Geophysical Research Letters, 30, https://doi.org/10.1029/2002gl016182, 2003.

King, M. A., Penna, N. T., Clarke, P. J., and King, E. C.: Validation of ocean tide models around Antarctica using onshore GPS and gravity data, Journal of Geophysical Research-Solid Earth, 110, https://doi.org/Artn B08401 10.1029/2004jb003390, 2005.

Kouba, J.: A guide to using International GNSS Service (IGS) Products, Report, Geodetic Survey Division, Natural Resources Canada, 2009.

Lau, H. C. P., Mitrovica, J. X., Davis, J. L., Tromp, J., Yang, H. Y., and Al-Attar, D.: Tidal tomography constrains Earth's deep-mantle buoyancy, Nature, 551, 321–326, https://doi.org/10.1038/nature24452, 2017.

Lyard, F., Lefevre, F., Letellier, T., and Francis, O.: Modelling the global ocean tides: modern insights from FES2004, Ocean Dynamics, 56, 394–415, https://doi.org/10.1007/s10236-006-0086-x, 2006.

Martens, H. R., Simons, M., Owen, S., and Rivera, L.: Observations of ocean tidal load response in South America from subdaily GPS positions, Geophysical Journal International, 205, 1637–1664, https://doi.org/10.1093/gji/ggw087, 2016.

Penna, N. T., Clarke, P. J., Bos, M. S., and Baker, T. F.: Ocean tide loading displacements in western Europe: 1. Validation of kinematic GPS estimates, Journal of Geophysical Research-Solid Earth, 120, 6523–6539, https://doi.org/10.1002/2015jb011882, 2015.

Petit, G. and Luzum, B., eds.: IERS Conventions, Verlag des Bundesamts für Kartographie und Geodäsie, Frankfurt am Main, 2010.

Schenewerk, M. S., Marshall, J., and Dillinger, W.: Vertical Ocean-loading Deformations Derived from a Global GPS Network, Journal of the Geodetic Society of Japan, 47, 237–242, https://doi.org/10.11366/sokuchi1954.47.237, 2001.

Stammer, D., Ray, R. D., Andersen, O. B., Arbic, B. K., Bosch, W., Carrère, L., Cheng, Y., Chinn, D. S., Dushaw, B. D., Egbert, G. D., Erofeeva, S. Y., Fok, H. S., Green, J. A. M., Griffiths, S., King, M. A., Lapin, V., Lemoine, F. G., Luthcke, S. B., Lyard, F., Morison, J., Müller, M., Padman, L., Richman, J. G., Shriver, J. F., Shum, C. K., Taguchi, E., and Yi, Y.: Accuracy assessment of global barotropic ocean tide models, Reviews of Geophysics, 52, 243–282, https://doi.org/10.1002/2014rg000450, 2014.

Susnik, A., Dach, R., Villiger, A., Maier, A., Arnold, D., Schaer, S., and Jäggi, A.: CODE reprocessing product series, CODE_REPRO_2015, https://doi.org/10.7892/boris.80011, http://ftp.aiub.unibe.ch/REPRO_2015/, 2016.

Thomas, I. D., King, M. A., and Clarke, P. J.: A comparison of GPS, VLBI and model estimates of ocean tide loading displacements, Journal of Geodesy, 81, 359–368, https://doi.org/10.1007/s00190-006-0118-9, 2006.

Urschl, C., Dach, R., Hugentobler, U., Schaer, S., and Beutler, G.: Validating ocean tide loading models using GPS, Journal of Geodesy, 78, 616–625, https://doi.org/10.1007/s00190-004-0427-9, 2005.

Wang, J., Penna, N. T., Clarke, P. J., and Bos, M. S.: Asthenospheric anelasticity effects on ocean tide loading around the East China Sea observed with GPS, Solid Earth, 11, 185–197, https://doi.org/10.5194/se-11-185-2020, 2020.

Wenzel, H.-G.: The nanogal software : Earth tide data processing package ETERNA 3.30, Bull. Inf. Marées Terrestres, 124, 9425–9439, 1996.

Yuan, L. G. and Chao, B. F.: Analysis of tidal signals in surface displacement measured by a dense continuous GPS array, Earth and Planetary Science Letters, 355-356, 255–261, https://doi.org/10.1016/j.epsl.2012.08.035, 2012.

Yuan, L. G., Chao, B. F., Ding, X., and Zhong, P.: The tidal displacement field at Earth's surface determined using global GPS observations, Journal of Geophysical Research: Solid Earth, 118, 2618–2632, https://doi.org/10.1002/jgrb.50159, 2013.

Zumberge, J. F., Heflin, M. B., Jefferson, D. C., Watkins, M. M., and Webb, F. H.: Precise point positioning for the efficient and robust analysis of GPS data from large networks, Journal of Geophysical Research: Solid Earth, 102, 5005–5017, https://doi.org/10.1029/96jb03860, 1997.